THE METEOROLOGICAL MAGAZINE

HER MAJESTY'S STATIONERY OFFICE

August 1980

Met.O. 931 No. 1297 Vol. 109

METEOROLOGICAL OFFICE Met.O.931

THE METEOROLOGICAL MAGAZINE

No. 1297, August 1980, Vol. 109

551.507.352:551.508.21

An aircraft-mounted pyranometer

By A. P. Cluley and J. P. Cowley

(Meteorological Office, Bracknell)

Summary

The installation of an upward-facing pyranometer on the Hercules aircraft of the Meteorological Research Flight is described. High-quality data have been obtained which permit detailed study to be made of both the horizontal and vertical variations of solar irradiance. As an illustration, data are presented from a flight on an occasion of a marked thermal inversion. Values of the turbidity coefficient proposed by Unsworth and Monteith are derived and the horizontal and vertical variations in these are examined.

Introduction

The ability to measure solar irradiances from an aircraft allows the spatial distribution of solar irradiance to be investigated in a variety of meteorological conditions. It also allows the contribution that the absorption of solar energy makes to the heat budget of clouds (e.g. stratocumulus) and that of the boundary layer to be estimated.

In this paper, the installation of an upward-facing pyranometer on the Hercules aircraft of the Meteorological Research Flight (MRF) is described. Some illustrative results from this instrument above and below a haze layer are presented only to demonstrate that the equipment is capable of giving measurements of high quality and of yielding some interesting results. Other radiation instruments (downward-facing pyranometer, upward- and downward-facing pyrgeometers) are currently being tested on the aircraft but these will not be discussed further here.

Pyranometers have been installed on earlier MRF aircraft (Roach, 1961) but the present installation yields more accurate results more readily as an instrument of superior performance has been used and the data from it are recorded on magnetic tape thus enabling subsequent computer processing.

General description and performance

An Eppley pyranometer (model PSP) has been installed on the top of the fuselage between the wings of the Hercules aircraft; see Plate I which is a photograph of the installation. This instrument is sensitive to radiation in the wavelength range 0·3 to 3 μm and has a time-constant of about 1 second.

It is mounted on a platform which is approximately level with respect to the aircraft reference axes and the whole assembly is exposed to the airflow during flight. A protective cover is fitted over the dome of the instrument when the aircraft is on the ground or during flights for which the instrument is not required. Exposure is good, although two parts of the aircraft, the tail and the radar pod, have had to be obscured from its field of view by installation of two matt-black obscurers. The effect of these on measurements is discussed later.

The output from the instrument is hard-wired into a head amplifier contained in a unit just inside the aircraft skin near the instrument. This unit also contains the electronics associated with a thermistor which is used to monitor the temperature of the instrument housing. The signal and temperature are sampled at 1 s^{-1} and 0·25 s^{-1} respectively. The gain and zero offset of the head amplifier can be monitored in flight by switching two precision voltages across the input in place of the pyranometer output. The instrument and electronics have performed well and the intrinsic noise level in the system is less than ± 1 bit on the data recording system ($= \pm 0{\cdot}7$ W m^{-2}). The gain and zero offset of the head amplifier are very stable though they are slightly temperature dependent, the gain varying by less than 1 per cent over the range of temperature (—40 °C to +20 °C) experienced under normal operating conditions.

The sensitivity of the instrument itself is dependent on its temperature but as this is measured, a correction can be applied. However, misleading results can be obtained under non-equilibrium conditions when the temperature of the instrument is changing.

Determination of radiation flux density

To determine radiation flux densities (irradiances) the absolute calibration, its dependence on instrument temperature and the calibration of the electronics must be known.

The instrument was originally calibrated in December 1975 by the manufacturer at a temperature of 25 °C by comparison with standard instruments which can be referred to the International Pyrheliometric Scale 1956, and it is this calibration that is used in this paper. Future calibrations will be carried out annually by the Meteorological Office at Bracknell, where outdoor comparisons with a standard pyrheliometer will be made.

To study the effect of temperature on the sensitivity of the instrument, it was exposed to a constant source of light from a xenon arc lamp and its output monitored as the temperature was changed. However, to obtain meaningful results a number of points had to be watched:

(1) The stability of the lamp output was checked and was found to vary by less than 0·5 per cent after an initial warm-up period of two hours.

(2) The optical arrangement was such that a uniform beam of light was incident on the instrument. Hence small variations in alignment caused by temperature changes could not significantly affect the instrument output.

(3) The instrument and head amplifier were housed in a vacuum chamber to prevent the optics being degraded by condensation.

(4) The gain and offset of the head amplifier were regularly measured throughout the experimental runs.

(5) Readings were taken only during periods when the temperature of the instrument was stable.

The results are illustrated in Figure 1, where the output voltage corrected for amplifier drifts is plotted against instrument temperature. Each run took a day. The arrows indicate the direction of temperature change between the individual measurements. Most of the scatter in this diagram probably arises from fluctuations ($\approx 0{\cdot}5$ per cent) in the lamp output during individual runs and differences in

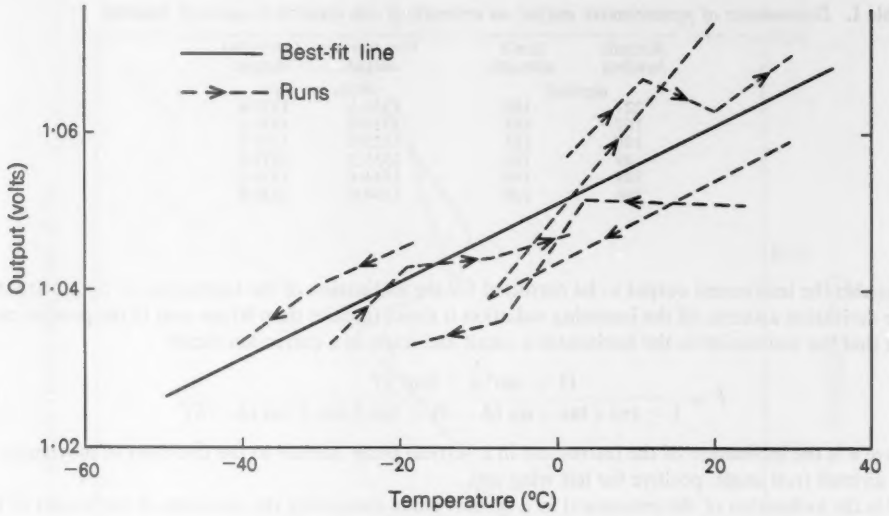

Figure 1. Variation of pyranometer output with instrument temperature.

its mean output from run to run. However, a clear trend emerges and the best-fit line for the variation of the output of the instrument with temperature is illustrated. This may be transformed to give the instrument sensitivity relative to the value at 25 °C (the manufacturer's calibration temperature):

$$S = S_{25}\{1 + \gamma\,(T - 25)\},$$

where S (V W^{-1} m^2) is the sensitivity at T °C, S_{25} is the sensitivity at 25 °C and $\gamma = 0{\cdot}00047$ K^{-1}. There is no systematic difference between the measurements taken when the temperature was increasing and those taken when it was decreasing.

Interpretation of measurements

We now consider the effect of the obscurers. The solid angles subtended at the detector by the fin and radome obscurers are 0·10 and 0·04 sr respectively (i.e. 2·2 per cent of the field of view has been obscured). However, if the radiation field is isotropic, then by use of the cosine law it is estimated that about 99 per cent of the true amount of radiation will be incident on the dectector. Thus if the incident radiation is predominantly diffuse, the effect can be removed by multiplying the data by a factor of 1·01. However, if it is predominantly direct, then no correction is necessary for the effect of the obscurers.

In level flight the aircraft flies with its nose up, so the inclination of the instrument with respect to the sun depends on the aircraft heading. This was investigated by flying six runs at 60° intervals in heading at a height of 3 km in cloudless conditions. The pyranometer output was averaged over two-minute runs (i.e. 120 samples) and these results are presented in Table I. An expression can be derived

Table I. *Dependence of pyranometer output on azimuth of sun relative to aircraft heading*

Aircraft heading	Sun's azimuth	Pyranometer output	Corrected output
degrees		*arbitrary units*	
227	182	1330·5	1332·6
167	183	1316·6	1330·3
106	185	1327·0	1335·7
49	186	1335·2	1332·6
348	188	1344·4	1330·3
286	190	1350·9	1340·8

to enable the instrument output to be corrected for the inclination of the instrument to the horizontal. The derivation assumes all the incoming radiation is direct (greater than 90 per cent in the present case) and that the inclination to the horizontal is small and leads to a correction factor

$$F = \frac{(1 + \tan^2\alpha + \tan^2\beta)^{\frac{1}{2}}}{1 + \tan\alpha \tan z \sin(\phi - \theta) - \tan\beta \tan z \cos(\phi - \theta)}, \qquad (1)$$

where α is the inclination of the instrument in a vertical plane normal to the direction of movement of the aircraft (roll angle, positive for left wing up),

β is the inclination of the instrument in a vertical plane containing the direction of movement of the aircraft (pitch angle, positive for nose up),

θ is the aircraft heading,

z is the solar zenith angle, and

ϕ is the azimuthal angle of the sun.

Two equations containing α and β may be obtained by use of data from the first four runs; solving gives

$$\alpha = -0{\cdot}6^\circ \quad \text{and} \quad \beta = 0{\cdot}8^\circ.$$

During these runs the aircraft's inertial navigation system indicated a mean aircraft roll angle of $-1{\cdot}1^\circ$ and a mean pitch angle of $3{\cdot}1^\circ$. Hence there must be offsets, $0{\cdot}5^\circ$ in roll and $2{\cdot}3^\circ$ in pitch, between the inclination of the pyranometer sensor and the reference levels of the inertial platform.

In Table I, corrected values are included which were derived using equation (1) and the values of α and β obtained above. The spread in these corrected values (ideally zero) is less than 1 per cent which is a third of that before corrections are applied. The residual spread is probably due to inaccurate determination of α and β and the fact that roll and pitch angles were not constant along each run. For flights in which the incident radiation is predominantly direct this correction factor may be used with the measured aircraft roll and pitch angles, incorporating the offsets derived above, to estimate the irradiance through a horizontal surface. If the radiation is mainly diffuse, no correction should be made.

Experimental flight

The first mission flown by the aircraft with the specific task of measuring global solar irradiance was carried out on 20 September 1977. Data were recorded for a series of straight and level runs in an area to the west of the Cornish coast, centred at 50°29′N 6°06′W. There was a 4 K inversion (see Figure 2) at a height of 1·8 km (830 mb), this level being well marked by the top of a haze layer. The area was cloud free apart from a few cumulus clouds which affected measurements on runs 2, 3 and 9.

A series of 10 runs was flown at 165 m above mean sea level (1015 mb), this being the lowest altitude

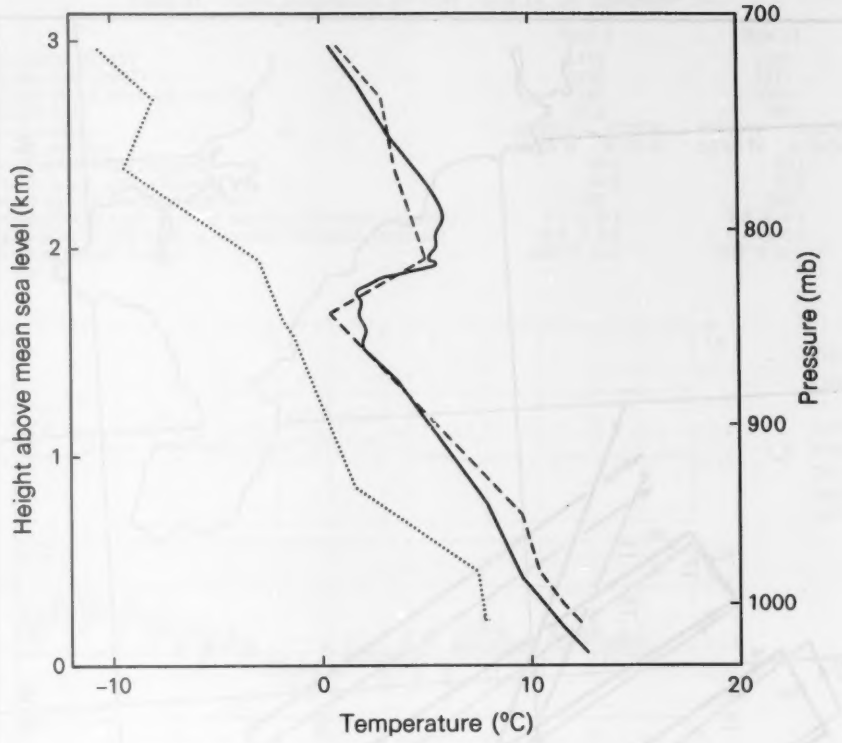

Figure 2. Temperature and humidity profiles on 20 September 1977.
– – – – – – – – – – – – Camborne 12 GMT dry-bulb temperatures.
..... Camborne 12 GMT dew-point temperatures.
——————— Aircraft temperatures.

considered safe for prolonged flight, and the pattern was repeated at 2060 m above mean sea level (789 mb), which was well above the inversion. The flight pattern is shown in Figure 3.

The effect of the inversion

The two diagonal runs (i.e. Nos. 1 and 11), details of which are summarized in Table II, have been chosen to illustrate the difference in the transmission of solar radiation above and below a well-defined inversion. The measurements of global irradiance for these runs are shown in Figure 4 before and after the application of equation (1) to correct for changes in the attitude of the aircraft, assuming

(a) roll and pitch angles measured by the aircraft's inertial platform, when corrected by the offsets derived above, refer to the plane of the sensing surface of the pyranometer, and

(b) the global radiation is predominantly direct.

It is suggested later that assumption (a) is not entirely correct. Figure 5 shows the standard deviation

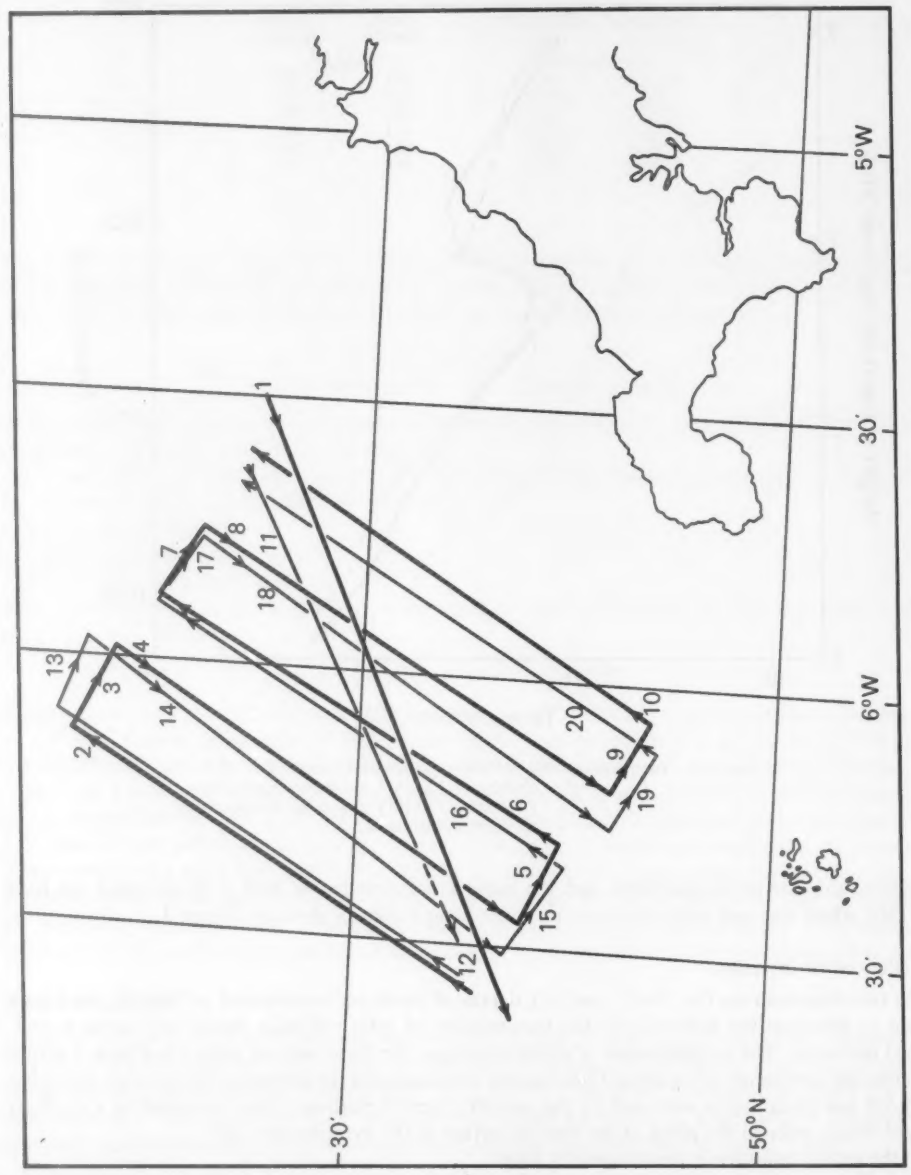

Figure 3. The flight pattern on 20 September 1977. Thin lines—high level (2060 m); thick lines—low level (165 m).

Table II. *Flight parameters for runs* 1 *and* 11, 20 *September* 1977

	Run 1	Run 11
Start time (GMT)	1118	1310
Finish time (GMT)	1130	1319
Height above mean sea level (m)	165	2060
Height (mb)	1015	789
Start position	50°40′N 5°20′W	50°40′N 5°20′W
Finish position	50°20′N 6°30′W	50°20′N 6°30′W
Start zenith angle (degrees)	50·5	52·1
Finish zenith angle (degrees)	49·7	51·9
Mean aircraft heading (degrees)	243	243
Mean aircraft pitch angle ± standard deviation (degrees)	2·1 ± 0·1	1·5 ± 0·1
Mean aircraft roll angle ± standard deviation (degrees)	0·4 ± 0·4	0·4 ± 0·3
Wind at aircraft height	090°/5 m s^{-1}	065°/6 m s^{-1}

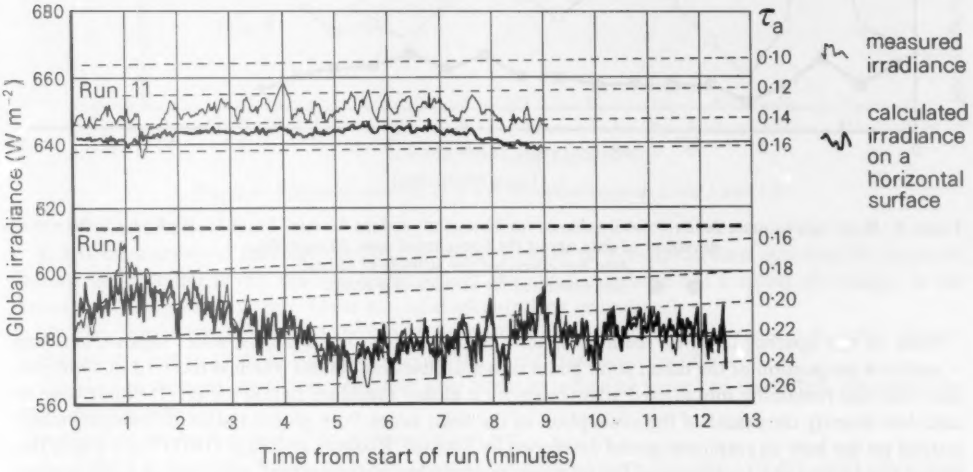

Figure 4. Global solar irradiance on a horizontal surface for runs 1 and 11.

of the data about linear trends for 30-second sections along each run, comparing the variation in the data before and after applying equation (1). It is clear from the diagram that changes in the aircraft's attitude are largely responsible for the fluctuations in the measured irradiances above the inversion, but rapid fluctuations remain in the data from below the inversion. It is suggested here that this is because

(a) the proportion of diffuse component in the global radiation at lower levels is larger, causing the correction for the aircraft's attitude (which assumes there to be only the direct component) to be less accurate, and

(b) there are small-scale variations in the turbidity of the air trapped in the haze layer.

The latter cause is thought to be the major one. The fluctuations in the data for run 11 after correction for the aircraft's attitude give a standard deviation of less than 1 W m^{-2}, which is the limit of resolution of the measuring system.

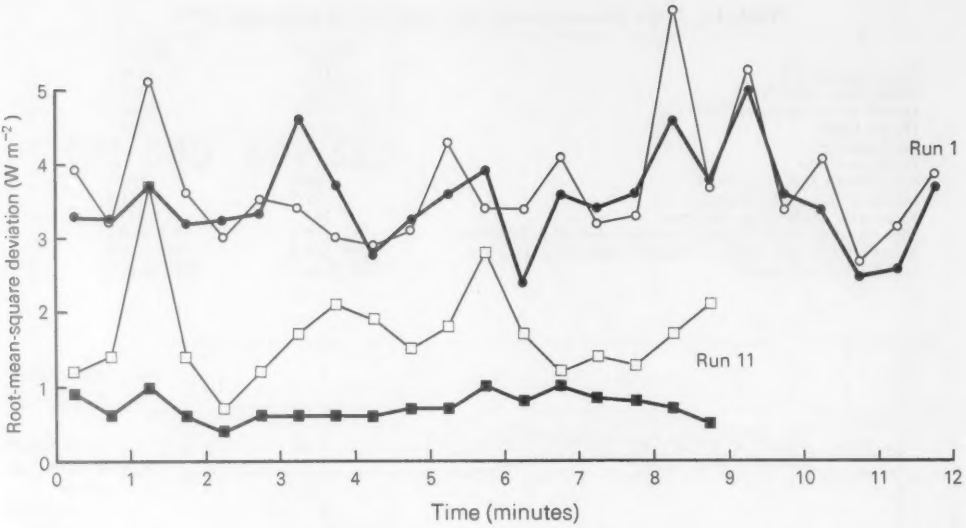

Figure 5. Root-mean-square deviation of irradiance for 30-second sections for runs 1 and 11. Each plot is the r.m.s. deviation of data about the linear trend over 30 seconds.
○ □ data not corrected for attitude of aircraft.
● ■ data corrected for attitude of aircraft.

Even in the absence of cloud the atmospheric components—air molecules, water vapour, aerosols—scatter a proportion of the direct solar beam into a diffuse component which is received in combination with the remaining unscattered solar beam by a global radiation pyranometer. It is not easy to calculate directly the extent of the absorption of the solar beam from global radiation measurements; instead we use here an empirical model developed by Souster, Rodgers and Page (1978) from which the global irradiances can be estimated for a known precipitable water content, solar zenith angle (which determine the air and water vapour mass along the beam) and turbidity. The turbidity coefficient used in this model is the τ_a proposed by Unsworth and Monteith (1972). They defined τ_a by

$$S(\tau_a) = S(0) \exp(-\tau_a m)$$

relating the measured flux at normal incidence $S(\tau_a)$ to the flux $S(0)$ calculated for a dust-free (but moist) atmosphere, when the optical air mass is m ($m \approx \sec z$). This turbidity coefficient is therefore a measure of the aerosol loading in the atmosphere.

Figure 4 shows isopleths of constant τ_a deduced from values of global radiation (corrected for the orientation of the pyranometer) using the model assuming values of precipitable water content calculated from the 12 GMT radiosonde ascent made from Camborne. Figure 6 shows the values of τ_a for each 30-second period of the two diagonal runs. It is evident that τ_a varied considerably during run 1 (below the inversion) ranging from 0·17 to 0·22, but there was much less change during run 11 (above the inversion) where τ_a was rather smaller, and only varied slightly between 0·15 and 0·16. It is suggested later that these longer-term changes in τ_a are correlated vertically and therefore are not a consequence of the inversion.

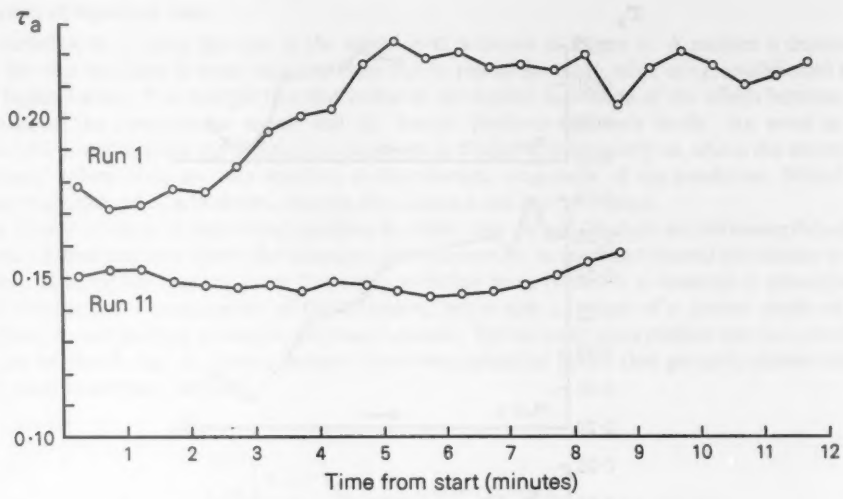

Figure 6. Turbidity coefficients τ_a for 30-second sections (runs 1 and 11).

It has been assumed that the precipitable water content of the atmosphere was sensibly constant during the experiment and that the variations of the irradiance were not a result of changes in the amount of precipitable water. These are valid assumptions because:

(a) The transmission of short-wave radiation through the atmosphere is insensitive to water vapour, a change of 1 mm in precipitable water altering the global irradiance by only 2 W m^{-2}.

(b) Marked changes in precipitable water only occur near frontal zones and there were none near the experimental area.

The effect of the inversion may be summarized to be:

(a) Global irradiances measured below the inversion are smaller (by about 20 per cent) than those measured above the inversion with corresponding differences of the reverse sign in the inferred turbidities.

(b) The existence of large-amplitude, high-frequency fluctuations in global irradiance (and hence in τ_a) below the inversion.

Comparison of low-level runs

In order to determine whether, at a fixed height, the longer-term changes in turbidity described above are spatial or temporal, values of τ_a have been estimated for runs 2, 4, 8 and 10 (run 6 was excluded because the data were unaccountably corrupted).

Figure 7 shows the variations in 30-second average turbidities for the four runs. The direction of time in the diagram depends on the run, the southern end of each run being to the left. Values of τ_a are not shown for sections in which data showed too great a variability to make a value of τ_a meaningful. It is evident that τ_a decreases going northwards along each run and that there is a notable minimum about 1 minute from the northern end of each run. It appears, therefore, that there is a spatial correlation from run to run in the longer-term variation in τ_a.

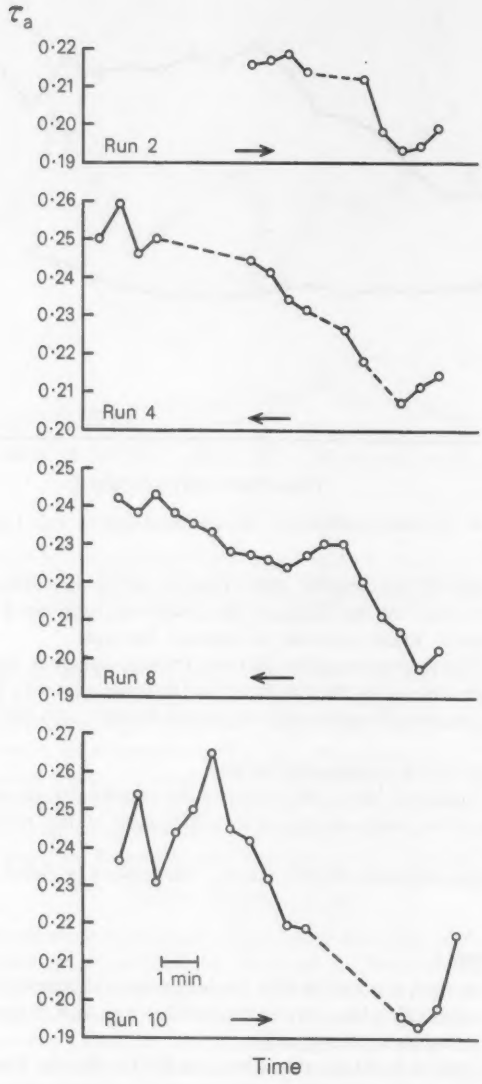

Figure 7. Turbidity coefficients τ_a for 30-second sections (runs 2, 4, 8 and 10).

Comparison of high-level runs

The variation in τ_a along the runs at the higher level is shown in Figure 8. A pattern is detectable among the runs but there is some variation from run to run in the mean value of τ_a, southbound runs having higher values. It is thought that this is due to the inexact derivation of the offsets between the orientation of the pyranometer sensor and the inertial platform reference levels. An error in the offsets of 0·3° could explain the discrepancy apparent in Figure 8, particularly as, above the inversion, the deduced values of τ_a are very sensitive to the absolute magnitude of the irradiance. Whilst the absolute magnitude of τ_a is in doubt, changes of τ_a along a run can be studied.

Runs 12 and 14 show τ_a decreasing northwards, while runs 18 and 20 show an increasing fall-off to the south. Therefore, even above the inversion there appears to be moderate spatial correlation in the turbidity. This implies that the lower frequency variation in τ_a (which is a measure of atmospheric aerosol only) is not a consequence of the inversion, but is also a feature of a greater depth of the atmosphere, caused perhaps by remote sources of aerosol. The air mass being studied here had travelled across the Midlands and the Severn Estuary (including industrial plants that generate plumes rich in aerosol, such as sulphur particles).

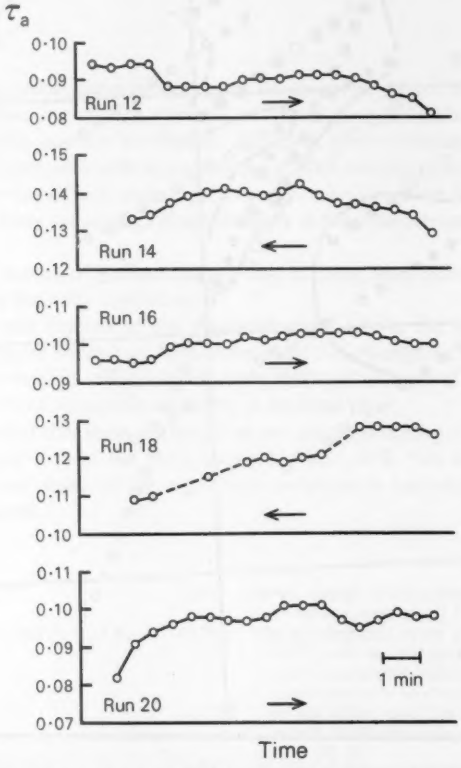

Figure 8. Turbidity coefficients τ_a for 30-second sections (runs 12, 14, 16, 18 and 20).

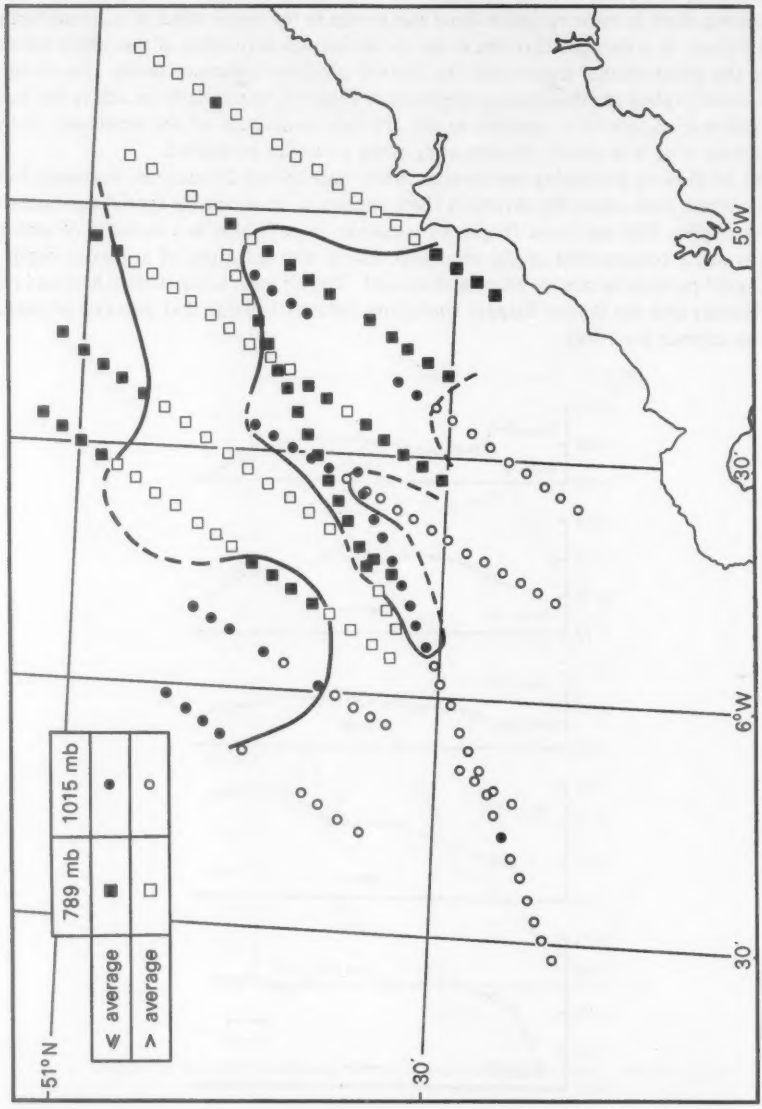

Figure 9. Map showing horizontal variations in turbidity at 1117 GMT on 20 September 1977. Locations are referred to 1117·53 GMT. It is assumed that the air moved at a speed of 6·5 m s^{-1} from a direction 065° east of north.

The possibility that the variations in τ_a discussed above result from the presence of variable amounts of cirrus cloud has been discounted as no cirrus was observed throughout the flight. Furthermore, the arrival at and the departure from the experimental area were made at high levels (greater than 6 km) at which cirrus cloud is more readily discernible.

Comparison of low- and high-level spatial variability in turbidity

Until an accurate correction for sensor orientation is determined it will not be possible to consider this topic in detail. However, a preliminary comparison has been made to see if the changes in τ_a along the runs at low and high level are associated. In this, the turbidities along each run were expressed as fractions of the average turbidity for that run. Figure 9 shows the result, assuming the whole of the air to move at 6·5 m s^{-1} from 065° east of north. All locations in the diagram refer to the position of that part of the air at the start of the experiment. Regions of 'higher than average' and 'lower than average' turbidity do associate reasonably well, supporting the suggestion made above that the low-frequency variations in τ_a are largely spatial. Also, these changes appear to persist throughout the experiment and are present both above and below the inversion and, hence, are not solely a feature of the haze layer.

Conclusions

The installation of an upward-facing pyranometer on the MRF Hercules has been described and sample data presented. These are of high quality and should permit detailed study of both the horizontal and vertical variation in solar irradiance. However, there remains an uncertainty as to the precise orientation of the instrument with respect to the aircraft reference axes. The effect of a marked thermal inversion has been considered and a number of conclusions have been drawn, although it is not known whether or not these are of general applicability as the results from only one flight have been examined:

(1) The irradiance level increased by about 20 per cent in going from below to above the inversion, as a result of the change in turbidity coefficient.

(2) Rapid fluctuations were present in the measurements. Above the inversion these have been shown to result from changes in aircraft attitude rather than real changes in irradiance. The data from measurements below the inversion still exhibited rapid fluctuations even after correction for aircraft attitude and are thus a result of changes in turbidity in the haze layer.

(3) It has been demonstrated that there are longer-term variations during the runs which are spatially correlated not only amongst runs at the same height but also with runs at the other measurement height. So, over a distance of about 60 km, significant variations in turbidity, not connected with the haze layer, have been detected.

References

Roach, W. T. 1961 Some aircraft observations of fluxes of solar radiation in the atmosphere. *Q J R Meteorol Soc*, **87**, 346–363.

Souster, C. G., Rodgers, G. G. and Page, J.K. 1978 The development of an interactive computer program SUN3 for the calculation of solar irradiances and daily irradiations incident upon surfaces of any slope and orientation on cloudless days for given conditions of sky clarity and atmospheric water content. University of Sheffield, Department of Building Science, *Note* BS 30.

Unsworth, M. H. and Monteith, J. L. 1972 Aerosol and solar radiation in Britain. *Q J R Meteorol Soc*, **98**, 778–797.

551.525.2(420)

An investigation into the variations of grass-minimum depressions

By M. N. Pickup
(Manchester Weather Centre)

Summary

The mean difference between screen-minimum and grass-minimum temperatures for both clear and cloudy nights was investigated for several stations in England. Little significant variation during cloudy nights was found. With clear skies and light winds the station-to-station variations were significant and it is suggested that they were due not only to differing site surroundings but perhaps also to different characteristics of the surface layers of the ground.

Introduction

Pickup (1976) showed that, during clear nights at West Raynham, mean values of the difference (Δ) between the screen-minimum and the grass-minimum temperatures decreased with increasing wind speed and also that little variation of Δ with wind speed occurred during cloudy nights. These results were generally significantly different from those of Craddock and Pritchard (1951) and Saunders (1952) for other locations.

The present investigation was carried out to check whether results similar to those obtained at West Raynham could be found at other stations.

Data

The locations of the stations selected are shown in Figure 1. The selection was limited to stations which had hourly or three-hourly observations on magnetic tape for the period under investigation (January 1961–December 1969).

Figure 1. Location of stations referred to in the text.

A computer program was used to extract dates of 'clear' and 'cloudy' nights. A 'clear' night was defined as one with less than 2/8 low cloud, medium cloud, or low and medium cloud combined at each available (hourly or three-hourly) observation between 21 and 09 GMT. Nights with cirriform cloud were included but nights when fog formed were excluded. A 'cloudy' night was defined as one with 8/8 low cloud, medium cloud, or low and medium cloud combined at each available observation between 21 and 09 GMT (excluding nights with precipitation). For each event the average wind speed overnight was computed and the difference (Δ) between the screen-minimum and the grass-minimum temperatures extracted.

The rigid criteria specified to the extraction program produced far fewer events at all the stations (except for clear nights with light winds at some stations) compared with the rather more flexible subjective method used when the original West Raynham observations were classified.

In the original selection of stations Shawbury was not included, but in order to increase the range of the investigation it was added for 'clear' nights only.

Results

The values of Δ for 'cloudy' nights were grouped according to mean surface wind speeds of 1–5, 6–10 and 11–15 knots. The results are shown in Table I. Only Chivenor and Stansted had more than five events in the 11–15 kn category, although even they fell far short of the numbers in the West Raynham sample because there were often brief clear intervals which the objective analysis rejected on otherwise cloudy nights. The totals of cloudy nights for all wind speeds at Boscombe Down (27) and Ringway (28) may seem low for data for a nine-year period, but for these stations cloud amounts and weather were checked for each hour whilst for the other stations they were checked only at three-hourly intervals. The results accorded well with those found at West Raynham, almost all values of Δ being less than 1 K.

Table I. *Depression (Δ) of grass-minimum temperature below screen-minimum temperature on nights with 8/8 low and/or medium cloud*, 1961–69

	Average overnight wind speed											
	1–5 knots				6–10 knots				11–15 knots			
	Mean	S.D.	*n*	S.E. of mean	Mean	S.D.	*n*	S.E. of mean	Mean	S.D.	*n*	S.E. of mean
	kelvins				*kelvins*				*kelvins*			
West Raynham	0·90	0·49	46	0·07	0·84	0·59	117	0·05	0·70	0·50	80	0·06
Boscombe Down	0·86	0·60	19	0·14	0·53	0·38	8	0·13	—			
Chivenor	1·43	1·02	26	0·20	0·83	0·81	25	0·16	1·28	1·56	6	0·64
Gatwick	0·92	0·92	30	0·17	0·88	0·80	17	0·19	—			
Ringway	0·62	0·64	18	0·15	0·48	0·18	10	0·06	—			
Stansted	0·99	0·94	14	0·25	0·71	0·80	24	0·16	1·07	0·93	8	0·33

S.D. = Standard deviation *n* = number of occasions S.E. = Standard error

Similar classifications of Δ for clear nights are shown in Table II. Although West Raynham, Boscombe Down, Stansted and Shawbury show a gradual decrease of Δ with increasing wind speeds the values at Chivenor, Gatwick and Ringway show a maximum Δ at the central (6–10 kn) range of wind speeds. This maximum is only statistically significant, however, (at the 5 per cent level) at Gatwick.

Table II. *Depression* (Δ) *of grass-minimum temperature below screen-minimum temperature on nights with less than* 2/8 *low and/or medium cloud,* 1961–69

	Average overnight wind speed											
	1–5 knots				6–10 knots				11–15 knots			
	Mean	S.D.	*n*	S.E. of mean	Mean	S.D.	*n*	S.E. of mean	Mean	S.D.	*n*	S.E. of mean
	kelvins				*kelvins*				*kelvins*			
West Raynham	5·34	1·03	118	0·09	3·71	1·17	327	0·06	2·08	0·51	135	0·04
Boscombe Down	4·52	1·39	95	0·14	3·11	1·45	65	0·18	2·58	1·36	29	0·25
Chivenor	3·33	1·34	104	0·13	3·51	1·42	65	0·18	3·10	1·26	17	0·31
Gatwick	3·29	1·09	137	0·09	4·04	1·21	39	0·19	2·87	0·51	7	0·19
Ringway	2·94	1·16	82	0·13	2·98	1·16	49	0·17	2·52	0·95	5	0·42
Stansted	4·86	1·51	96	0·15	3·34	1·34	102	0·13	2·33	0·77	17	0·19
Shawbury	5·12	1·04	105	0·10	4·68	1·22	32	0·22	3·47	0·75	8	0·27

S.D. = Standard deviation *n* = number of occasions S.E. = Standard error

Discussion

Student's *t*-tests were made on the differences between the means for the various stations on cloudy nights. The results are shown in Table III. Against each station are listed those other stations which showed no significant difference between the means (probability $P = 5$ per cent) for each wind-speed category. In each of the 1–5 kn and 6–10 kn categories, 12 out of 15 were not significantly different. None of the three samples with winds 11–15 kn were significantly different. Thus 27 out of a total of 33 tests showed no significant differences between the means. Similarly *t*-tests showed that few of the differences between these average values for different speed ranges for the same stations are statistically significant at the 5 per cent level. It seems therefore to be appropriate to suggest that a value of Δ of 0·9 K (or 1 K if working in whole degrees) would be suitable for all stations during cloudy nights irrespective of wind speed. However, if the differences found here are indeed representative true differences, then in view of the scatter in the results and the numbers of events involved, it should be realized that the odds in favour of failing to find statistically significant differences in these trials are nearly all well above evens—both for differences between stations for the same speed range and between speed ranges for the same stations. It has also to be remembered that Shawbury—the station where the combined effects of soil density, specific heat capacity and thermal conductivity differ most from those of the other stations (see below)—was not included in this investigation for cloudy nights.

Similarly, *t*-tests were carried out on the data for clear nights. The results are shown in Table IV. In the 1–5 kn category only 4 out of a total of 21 tests were not significantly different. This increased to 7 out of 21 in the 6–10 kn range and to 15 out of 21 with winds of 11–15 kn. These results indicate that in relation to the scatter of the data and the numbers of events involved in the analysis the effects of site differences become less important as the wind speed increases and that the inter-station differences apparent when winds are above 10 kn could, for the most part, arise readily enough by chance. Some comparisons involving West Raynham—where the number of events is much larger than elsewhere—and Shawbury—where mean values of Δ are high—provide notable exceptions. Thus Δ values for one site are likely to provide poor estimates of Δ for other locations in situations with light winds or clear skies. On some airfields the enclosure is surrounded by 'pans' (extensive areas of level concrete), taxi-ways and buildings, which may mean that with light winds cooling is reduced by conduction from the surroundings. Another factor, however, may be the variation in soil types on the sites.

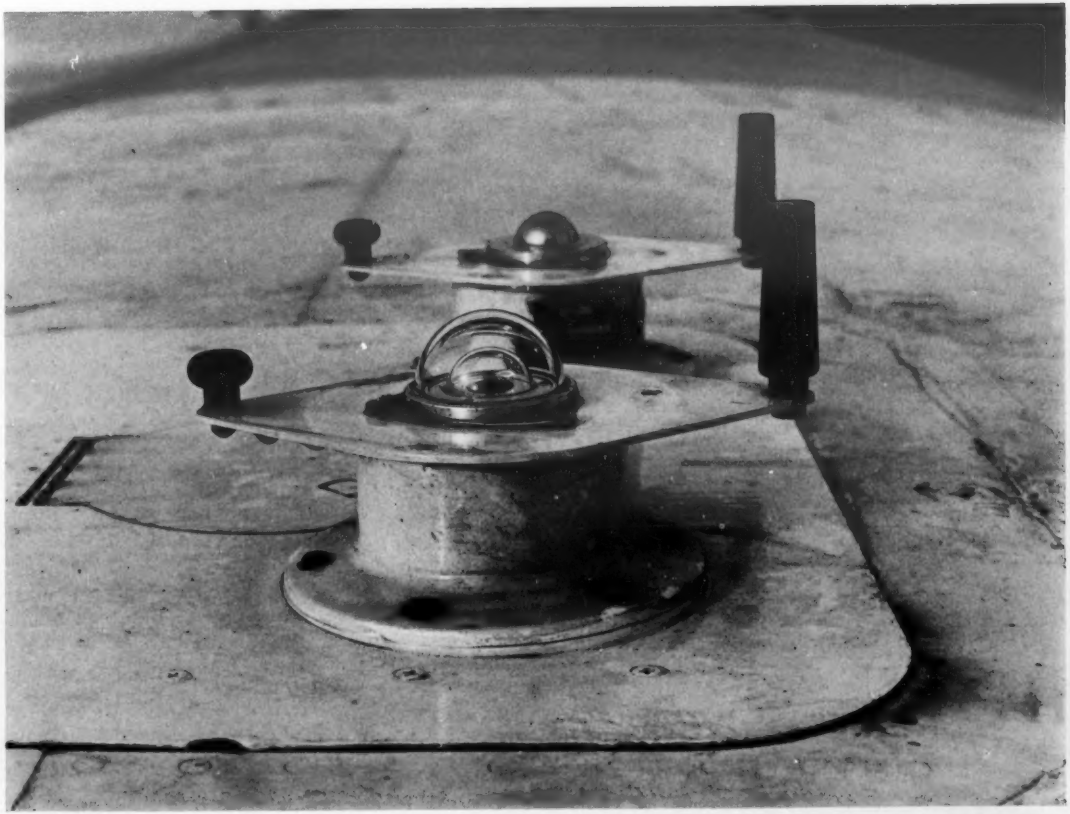

Plate I. An Eppley pyranometer installed on a Hercules aircraft of the Meteorological Research Flight. (See page 217.)

To face page 232

Plate II. General view of the Museum of Meteorological Instruments at Meteorological Office Headquarters, Bracknell. (See page 246.)

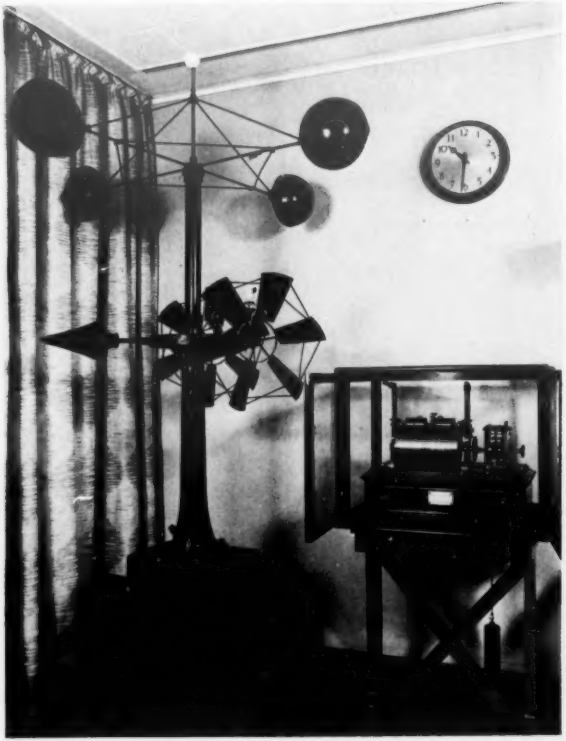

Plate III. Beckley–Robinson anemograph.

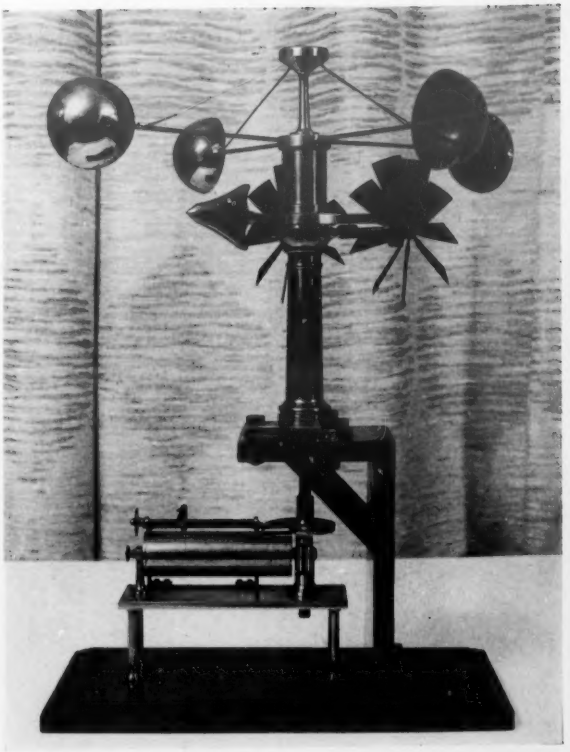

Plate IV. Prototype model wind vane constructed by Robert Beckley.

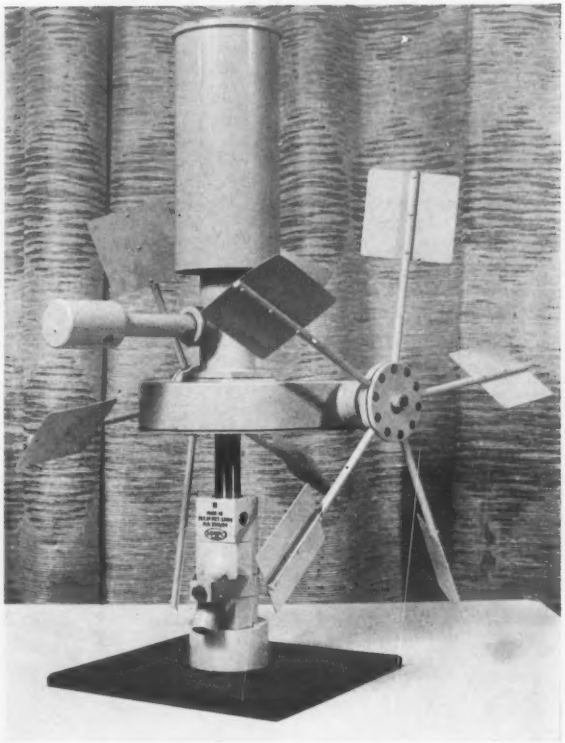

Plate V. Modern Mk 4E wind vane.

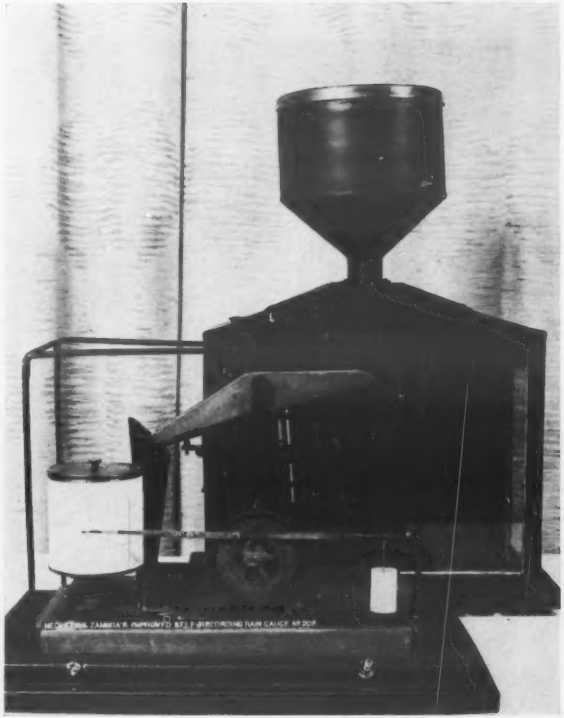

Plate VI. Negretti & Zambra improved self-recording rain-gauge (*c.* 1890).

Plate VII. Negretti & Zambra dial rain-gauge.

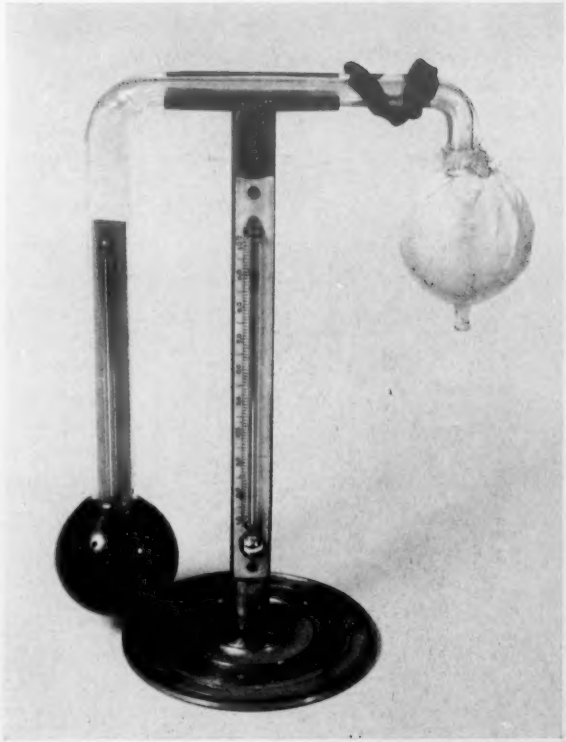

Plate VIII. Daniell's dew-point hygrometer (1860).

Plate IX. Kater's hygrometer (*c.* 1812).

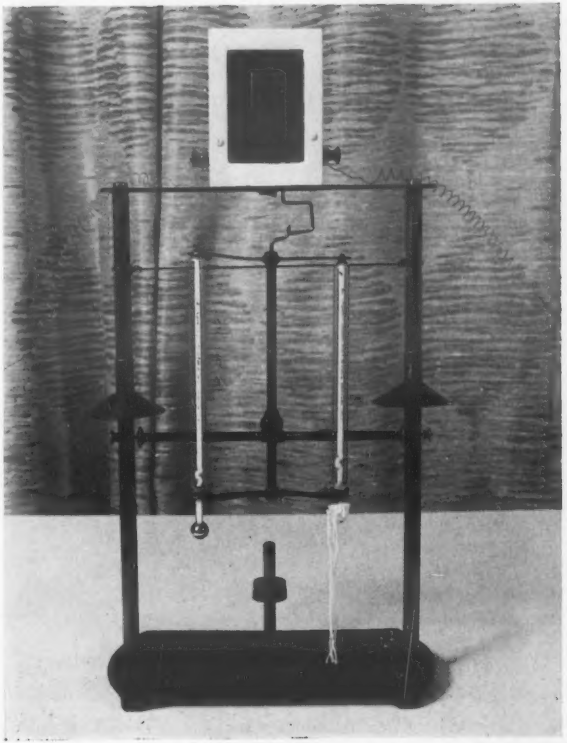

Plate X. Negretti & Zambra recording thermometer (*c.* 1898).

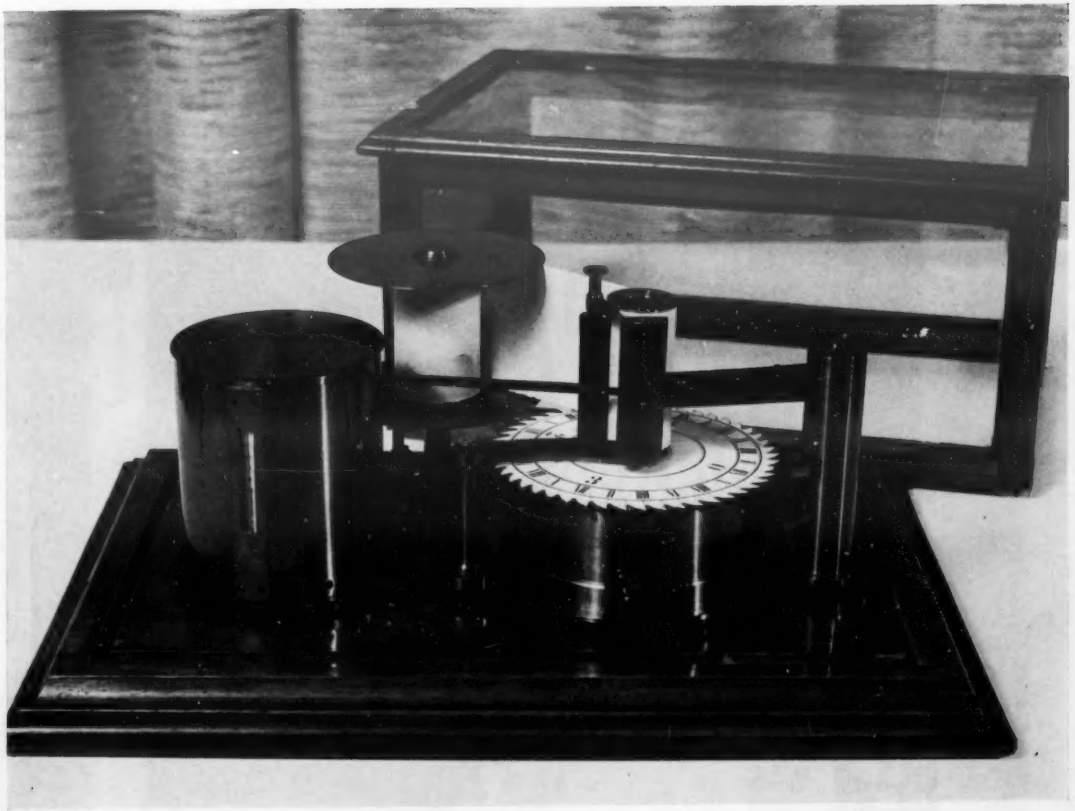

Plate XI. Goldschmid barograph (1880).

To face page 233

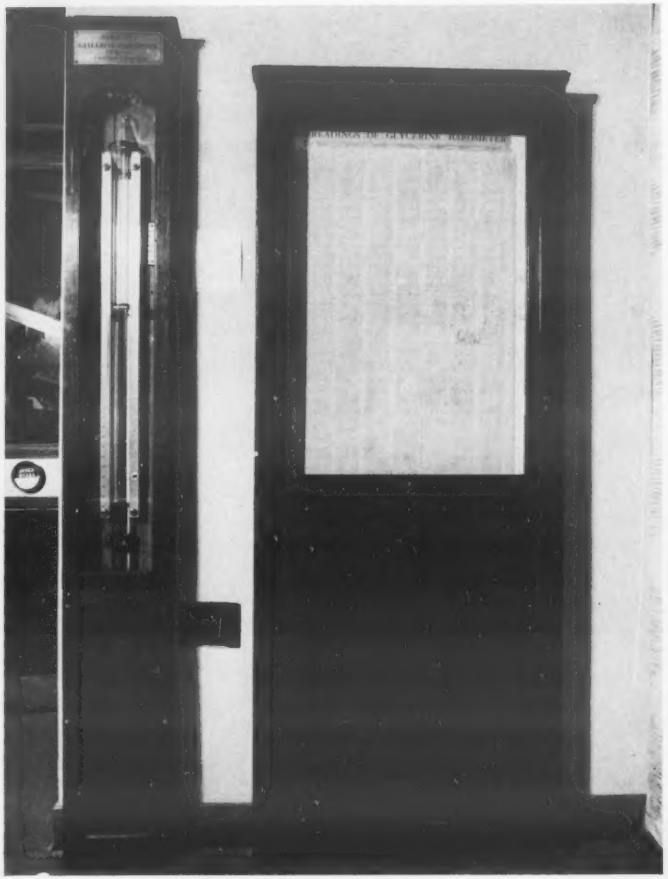

Plate XII. Top part of Jordan glycerine barometer.

Plate XIII. Mercury barometer by Dan Quare (*c.* 1695).

Table III. *Results of Student's* t*-tests to compare means of* Δ *against control stations during cloudy nights. Stations listed were not significantly different* ($P = 5$ *per cent*)

Control Station	Average wind speed 1–5 knots	6–10 knots	11–15 knots
West Raynham	Boscombe Down Gatwick Ringway Stansted	Chivenor Gatwick Stansted	Chivenor Stansted
Boscombe Down	West Raynham Gatwick Ringway Stansted	Chivenor Gatwick Ringway Stansted	*
Chivenor	Gatwick Stansted	West Raynham Boscombe Down Gatwick Stansted	West Raynham Stansted
Gatwick	West Raynham Boscombe Down Chivenor Ringway Stansted	West Raynham Boscombe Down Chivenor Ringway Stansted	*
Ringway	West Raynham Boscombe Down Gatwick Stansted	Boscombe Down Gatwick Stansted	*
Stansted	West Raynham Boscombe Down Chivenor Gatwick Ringway	West Raynham Boscombe Down Chivenor Gatwick Ringway	West Raynham Chivenor

* Boscombe Down, Gatwick and Ringway had no data with winds 11–15 knots.

Effect of soil type

Brunt (1939) showed that, in general, turbulence is a far more effective agent than radiation in transferring heat vertically through the atmosphere. But he also showed that at very small heights above the ground when turbulence is unable to develop effectively, the transfer of heat there is mainly by radiation. With simplifying assumptions, Brunt calculated that the nocturnal fall of temperature at the ground was proportional to the square root of the time from sunset and inversely proportional to $\rho ca^{\frac{1}{2}}$, where ρ is density, c specific heat capacity and a the thermal diffusivity of the ground. The fall of surface temperature over sandy soil, where for dry sand $(\rho ca^{\frac{1}{2}})^{-1} \approx 71$—a value which decreases rapidly as the water content is increased—should be greater than over concrete, where for concrete used in dams $(\rho ca^{\frac{1}{2}})^{-1} \approx 18$ (using values in appropriate units from the *Smithsonian meteorological tables*, 1958 edition, Table 122).

Zdunkowski and Trask (1971) applied a radiative–conductive numerical model to the simulation of nocturnal temperature change over four soil types for a night with clear skies and a constant gradient wind of 10 m/s (20 kn) (which led to 10 m winds of about 10 kn), and assuming no deposition of dew. From their graphs of cooling from sunset for the earth's surface (simulated roughness appropriate to short grass) and for 180 cm above the surface, values of the depression (D) of surface temperature

Table IV. *Results of Student's* t*-tests to compare means of* Δ *against control stations during clear nights. Stations listed were not significantly different* ($P = 5$ *per cent*)

Control station	Average wind speed 1–5 knots	6–10 knots	11–15 knots
West Raynham	Shawbury	Chivenor Gatwick	Boscombe Down Ringway Stansted
Boscombe Down	Stansted	Chivenor Ringway Stansted	West Raynham Chivenor Gatwick Ringway Stansted
Chivenor	Gatwick	West Raynham Boscombe Down Stansted	Boscombe Down Gatwick Ringway Shawbury
Gatwick	Chivenor	West Raynham	Boscombe Down Chivenor Ringway Stansted Shawbury
Ringway		Boscombe Down Stansted	West Raynham Boscombe Down Chivenor Gatwick Stansted Shawbury
Stansted	Boscombe Down Shawbury	Boscombe Down Chivenor Ringway	West Raynham Boscombe Down Gatwick Ringway
Shawbury	West Raynham Stansted		Chivenor Gatwick Ringway

below the temperature at 180 cm eight hours after sunset were estimated for their four soil types. These are shown in Table V together with associated values of $(\rho ca^{\frac{1}{2}})^{-1}$ for the soils they considered.

Details of the soil at the stations under investigation here were obtained from *Aerodrome weather diagrams and characteristics* and are shown in Table VI. They are unfortunately too vague to use for estimating values of $(\rho ca^{\frac{1}{2}})^{-1}$, and enclosures are not necessarily representative of the surrounding soil type—especially at Ringway. A comparison of the theoretical D with the observed Δ is difficult, especially since water content has a considerable effect. We can, however, try to estimate the range of

Table V. *Values of* $(\rho ca^{\frac{1}{2}})^{-1}$ *and the depression of surface temperature below that at the* 180 *cm level for various soil types*

Soil type	$(\rho ca^{\frac{1}{2}})^{-1}$ [$cm^2\ K\ s^{\frac{1}{2}}\ cal^{-1}$]	D after 8 hours *kelvins*
Quartz sand, medium fine dry	71	5·4
Sandy clay, 15 per cent moisture	28	3·2
Humus	25	2·9
Rocky soil	13	2·2

Values of D are derived from Figures 5 and 6 of Zdunkowski and Trask (1971) and represent the depression of surface temperature below that at a height of 180 cm 8 hours after sunset on a simulated clear night.

Table VI. *Details of the soil type at each station*

Station	Height above sea level *metres*	Soil type
West Raynham	78	Loamy soil covering clay with a chalk base
Boscombe Down	124	Chalk downland
Chivenor	8	Alluvial clay—not well drained
Gatwick	59	Clay subsoil—holds water near the surface
Ringway	78	Sand and clay loam
Stansted	106	Subsoil, heavy clay—poor drainage
Shawbury	76	Sand and gravel loam

$(\rho c a^{\frac{1}{2}})^{-1}$ among stations assuming the theory to be correct. From Table II the range of Δ among stations for a 10 kn wind on clear nights, obtained by extrapolating between the ranges, is approximately 2·8 to 4·2 K. Assuming a 12-hour night and a $t^{\frac{1}{2}}$ cooling rate, this is equivalent to 2·3 to 3·4 K for an 8-hour cooling period, giving $(\rho c a^{\frac{1}{2}})^{-1}$ in the range 15 to 35 units. This range agrees fairly well with the values in Table V and suggests that better estimates of $(\rho c a^{\frac{1}{2}})^{-1}$ for individual sites might help in predicting Δ.

Some large observed values of Δ

With clear skies and light winds, heat transfer is mainly by radiation and large differences between screen and grass temperatures frequently occur shortly after sunset with a rapid fall of ground temperature. Several occasions when this occurred at West Raynham in 1973 and 1974 are listed in Table VII.

Table VII. *Observed values of Δ at West Raynham*

Date	Sunset (GMT)	Time (GMT)	Air min.	Grass min.	Δ
			degrees Celsius		*kelvins*
1.2.73	1645	18–21	1·3	—4·5	5·8
26.3.73	1823	19	7·4	—3·0	10·4
		18–21	3·3	—3·1	6·4
25.4.73	1914	18–21	5·0	—3·5	8·5
1.5.73	1928	22	6·9	—5·6	12·5
		23	5·8	—4·8	10·6
		21–09	2·0	—6·2	8·2
1.10.73	1738	18–21	6·9	1·5	5·4
23.10.73	1648	18–21	5·2	—1·0	6·2
20.11.73	1558	20	0·5	—5·9	6·4
		18–21	—0·1	—6·0	5·9
13.3.74	1759	18–21	2·8	—3·5	6·3
14.3.74	1802	18–21	0·8	—6·4	7·2
20 3 74	1812	18–21	5·1	—2·5	7·6
27.8.74	1901	19–21	10·5	3·5	7·0

When a range of times is given the temperatures recorded are each the minimum for that period. It is evident that on each of the three nights when temperatures for more than one period were recorded, although both air temperatures and the grass temperatures continued to fall, the values of Δ decreased as time passed. This implies that Δ based upon night minima will be less than values for Δ experienced early in the night.

Before January 1978 grass minimum temperatures were officially recorded between 21 and 09 GMT. During trials at Porton Down in April 1977 a continuous trace of air temperature and grass-minimum depression was obtained for several nights, between 18 and 06 GMT, using platinum resistance thermometers. The results for periods ending at 05 GMT for two clear nights with light winds, 4/5 April and

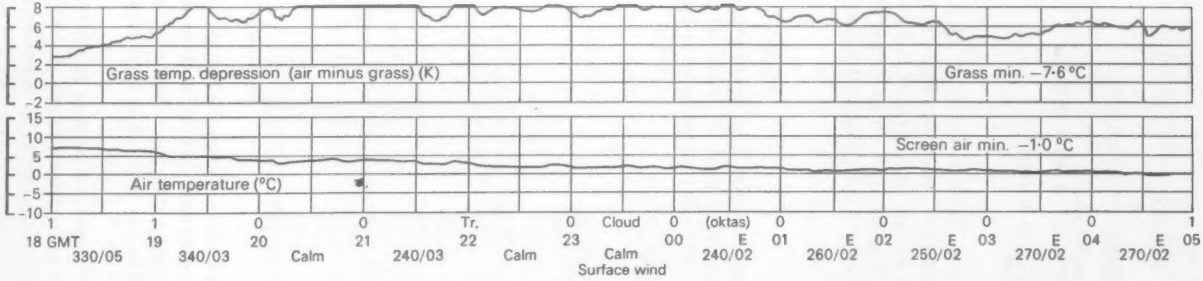
Grass temp. depression (air minus grass) (K)
Grass min. −7·6 °C
Screen air min. −1·0 °C
Air temperature (°C)
18 GMT 19 20 21 22 23 00 01 02 03 04 05
330/05 340/03 Calm 240/03 Calm Calm 240/02 260/02 250/02 270/02 270/02
Surface wind

Figure 2. Diagrammatic representation of air temperature and grass-temperature depression recorded at Porton Down between 18 GMT on 4 April 1977 and 05 GMT on 5 April 1977 (sunset 1844 GMT).

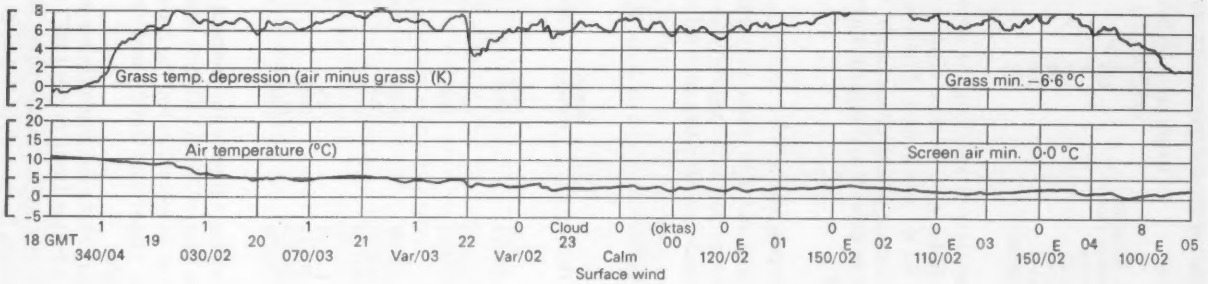
Grass temp. depression (air minus grass) (K)
Grass min. −6·6 °C
Air temperature (°C)
Screen air min. 0·0 °C
18 GMT 19 20 21 22 23 00 01 02 03 04 05
340/04 030/02 070/03 Var/03 Var/02 Calm 120/02 150/02 110/02 150/02 100/02
Surface wind

Figure 3. Diagrammatic representation of air temperature and grass-temperature depression recorded at Porton Down between 18 GMT on 15 April 1977 and 05 GMT on 16 April 1977 (sunset 1902 GMT).

15/16 April, are shown in Figures 2 and 3. On both occasions the value of Δ overnight was 6·6 K although depressions of 8 K occurred within an hour of sunset. In fact, on the 15th a depression of 6 K was recorded at sunset (1902 GMT). This is an important factor, especially during the winter months, when considering the possibility of ground frost.

Conclusions

For cloudy nights a value of screen-minimum minus grass-minimum temperature (Δ) equal to about 0·9 K applies to the different sites considered, irrespective of wind speed overnight.

For clear nights the value of Δ usually decreases with increasing wind speed but variations occur, especially with light winds, probably owing both to local site characteristics and to the effects of the various soil types.

With clear skies and light winds large depressions of grass temperature below the screen temperature frequently occur shortly after sunset. These depressions are often several degrees larger than values of Δ based upon night minimum temperatures, and are more likely to occur when the soil is dry, since $(\rho c a^{\frac{1}{2}})^{-1}$ decreases with increasing water content. Under similar conditions, large differences can also be expected between grass-minimum and concrete-minimum temperatures.

Acknowledgements

The author would like to thank Mr C. L. Hawson and other members of the staff of the Outstations Investigations Section of the Special Investigations Branch of the Meteorological Office for help in the preparation of this paper.

References

Brunt, D. 1939 Physical and dynamical meteorology, second edition. London, Cambridge University Press.

Craddock, J. M. and Pritchard, D. 1951 Grass minimum temperatures on nights without fog. *Meteorol Res Pap* No. 624. (Unpublished, copy available in the National Meteorological Library, Bracknell.)

Pickup, M. N. 1976 A statistical method of forecasting grass-minimum temperatures at West Raynham. *Meteorol Mag*, **105**, 122–127.

Saunders, W. E. 1952 Some further aspects of night cooling under clear skies. *Q J R Meteorol Soc*, **78**, 603–612.

Zdunkowski, W. G. and Trask, D. C. 1971 Application of a radiative–conductive model to the simulation of nocturnal temperature changes over different soil types. *J Appl Meteorol*, **10**, 937–948.

551.501.4:551.571

Computation of vapour pressure, dew-point and relative humidity from dry- and wet-bulb temperatures

By G. P. Sargent
(Meteorological Office, Bracknell)

Summary

A current project in the Operational Instrumentation Branch (Met O 16) of the Meteorological Office, Bracknell, required the collation of procedures for computing atmospheric moisture variables from readings of dry- and wet-bulb temperatures. It was thought that such a collation would prove a useful addition to the literature. This paper, therefore, describes some of the procedures that are available.

Introduction

The dry- and wet-bulb psychrometer is one of the commonest instruments used for obtaining information about the moisture content of the atmosphere. It is a relatively simple instrument and, provided that precautions are taken to maintain the wet bulb properly, it is capable of giving good results.

One of the drawbacks is that the computations of vapour pressure, dew-point and relative humidity are complex and not easily achieved by the use of small electronic calculators or microprocessors.

This paper sets out various equations which may be used for these computations, with an indication of the accuracy of the computation relative to the Goff–Gratch formula.

The following details concerning the notation used in these equations should be noted: $\exp_{10}x \equiv 10^x$; 'lg' implies logarithm to base 10; 'ln' implies logarithm to base e.

Equations for saturation vapour pressure

Goff–Gratch. The Goff–Gratch equations (Goff and Gratch, 1945) are the bases of the tables of saturation vapour pressure published in the *Smithsonian meteorological tables* and of the Meteorological Office humidity slide-rule.

For saturation vapour pressure with respect to a plane surface of pure water,

$$\begin{aligned}\lg e_w = &-7{\cdot}90298(T_s/T - 1) + 5{\cdot}02808 \lg (T_s/T) - \\ &- 1{\cdot}3816 \times 10^{-7} [\{\exp_{10} 11{\cdot}344(1 - T/T_s)\} - 1] + \\ &+ 8{\cdot}1328 \times 10^{-3} [\{\exp_{10} - 3{\cdot}49149 (T_s/T - 1)\} - 1] + \lg e_{ws}, \quad .. \quad .. \quad (1)\end{aligned}$$

where e_w = saturation vapour pressure in millibars with respect to a plane surface of pure water at temperature T,
T = temperature in kelvins,
T_s = temperature at the steam-point (= 373·16 K), and
e_{ws} = saturation vapour pressure in millibars at the steam-point temperature (= 1013·246 mb).

For saturation vapour pressure with respect to a plane surface of pure ice,

$$\begin{aligned}\lg e_i = &-9{\cdot}0718(T_0/T - 1) - 3{\cdot}56654 \lg (T_0/T) + \\ &+ 0{\cdot}876793(1 - T/T_0) + \lg e_{i0}, \quad .. \quad .. \quad .. \quad .. \quad .. \quad .. \quad .. \quad (2)\end{aligned}$$

where e_i = saturation vapour pressure in millibars with respect to a plane surface of pure ice,
T = temperature in kelvins,
T_0 = temperature at the ice-point (= 273·16 K), and
e_{i0} = saturation vapour pressure in millibars at the ice-point temperature (= 6·1071 mb).

These equations are based on theoretical considerations and experimental data. Equation (1) is valid for temperatures between 0 °C and 100 °C and is accepted for temperatures between 0 °C and — 50 °C until further research indicates it to be in error. It should be noted that below 0 °C equation (1) relates to supercooled water. Equation (2) is valid for temperatures between 0 °C and — 100 °C.

The Goff–Gratch equations were formulated using the old Kelvin scale of temperature and the old definition of a standard atmosphere. Goff (1965) later transposed equations (1) and (2) to take into account the new Kelvin scale of temperature and the current definition of a standard atmosphere:

$$\begin{aligned}\lg (e_w/e_{ws}') = {} & 10{\cdot}79586(1 - T_{01}/T) - 5{\cdot}02808 \lg (T/T_{01}) + \\ & + 1{\cdot}50474 \times 10^{-4} [1 - \{\exp_{10} - 8{\cdot}29692(T/T_{01} - 1)\}] + \\ & + 0{\cdot}42873 \times 10^{-3} [\{\exp_{10} 4{\cdot}76955(1 - T_{01}/T)\} - 1] - \\ & - 2{\cdot}2195983, \quad .. \quad .. \quad .. \quad .. \quad .. \quad .. \quad .. \quad .. \end{aligned} \tag{3}$$

$$\begin{aligned}\lg (e_i/e_{ws}') = {} & - 9{\cdot}096936(T_{01}/T - 1) - 3{\cdot}56654 \lg (T_{01}/T) + \\ & + 0{\cdot}876817(1 - T/T_{01}) - 2{\cdot}2195983, \quad .. \quad .. \quad .. \quad .. \end{aligned} \tag{4}$$

where e_w and e_i are as in equations (1) and (2),

e_{ws}' = saturation vapour pressure in millibars at the steam-point temperature (new scale) (= 1013·25 mb),

T = temperature in kelvins (new scale), and

T_{01} = temperature of the triple point of water in kelvins (new scale) (= 273·16 K).

It should be noted that equations (3) and (4) give saturation vapour pressures differing from those given by equations (1) and (2) by amounts corresponding to temperature differences of less than 0·005 °C throughout the range — 100 °C to + 100 °C. The differences can thus be ignored for practical psychrometry.

The Goff–Gratch equations are generally accepted as giving the closest approximations to the true values of saturation vapour pressure, but they do not lend themselves to easy manipulation, especially if it is desired to find the temperature corresponding to a given value of saturation vapour pressure.

Various workers have approximated the Goff–Gratch relationship with expressions which are more amenable to automatic computation.

Hooper. During the development of the Meteorological Office Mk 3 radiosonde system, Hooper (unpublished working paper) developed a sixth-order polynomial to compute saturation vapour pressures with respect to a plane water surface. The coefficients were determined by Clenshaw's method of orthogonal polynomials (Clenshaw, 1960). It is claimed to be valid between — 40 °C and + 50 °C.

$$e_w = \exp (L_0 + L_1T + L_2T^2 + L_3T^3 + L_4T^4 + L_5T^5 + L_6T^6), \quad .. \quad .. \quad .. \tag{5}$$

where e_w = saturation vapour pressure in millibars with respect to a plane surface of pure water

T = temperature in degrees Celsius

L_0 = 1·809544921

L_1 = 7·266467428 × 10^{-2}

L_2 = — 2·996322270 × 10^{-4}

L_3 = 1·155167035 × 10^{-6}

L_4 = — 4·564108094 × 10^{-9}

L_5 = 2·687871955 × 10^{-11}

L_6 = — 1·603993935 × 10^{-13}.

Over the quoted range this has a maximum departure from Goff–Gratch at + 50 °C of — 8·63 × 10^{-3} mb.

Examination of the coefficients for Hooper's polynomial reveals that they can be adjusted to give a closer approximation to the Goff–Gratch results. Thus:

$L_0 = 1{\cdot}809567918$
$L_1 = 7{\cdot}266296315 \times 10^{-2}$
$L_2 = -2{\cdot}996403370 \times 10^{-4}$
$L_3 = 1{\cdot}160464233 \times 10^{-6}$
$L_4 = -4{\cdot}606513971 \times 10^{-9}$
$L_5 = 2{\cdot}315159066 \times 10^{-11}$
$L_6 = -1{\cdot}103513358 \times 10^{-13}$.

These coefficients give a maximum departure from Goff–Gratch of — 1·88 × 10^{-4} mb at + 50 °C over the range — 40 °C to + 50 °C.

Richards. Richards (1971) presented an equation to approximate the Goff–Gratch equation, claiming sufficient accuracy for most purposes. The coefficients have been adjusted to minimize the errors, using Powell's method (Powell, 1965).

$$e_w = e_{ws}' \exp(13{\cdot}3185t - 1{\cdot}9760t^2 - 0{\cdot}6445t^3 - 0{\cdot}1299t^4), \quad .. \quad .. \quad .. \quad (6)$$

where $t = (1 - T_s/T)$,
e_w = saturation vapour pressure in millibars with respect to a plane surface of pure water,
e_{ws}' = saturation vapour pressure in millibars at the steam-point temperature (new scale) (= 1013·25 mb),
T = temperature in kelvins (new scale), and
T_s = temperature at the steam-point (= 373·15 K).

Richards claims a normalized discrepancy of less than 0·001 between his formula and Goff–Gratch between — 50 °C and 140 °C. In the range — 40 °C to + 50 °C the maximum departure from Goff–Gratch is 1·611 × 10^{-2} mb at + 50 °C.

Lowe. Lowe (1977) presented a series of polynomials to approximate saturation vapour pressures. To achieve a similar degree of accuracy to Richards's method a sixth-degree polynomial is required. The coefficients were determined by means of a Chebyshev fitting procedure. For a temperature range — 50 °C to + 50 °C:

$$e_w = C_0 + C_1T + C_2T^2 + C_3T^3 + C_4T^4 + C_5T^5 + C_6T^6, \quad .. \quad .. \quad .. \quad (7)$$

where e_w = saturation vapour pressure in millibars with respect to a plane surface of pure water
T = temperature in degrees Celsius
$C_0 = 6{\cdot}107799961$
$C_1 = 4{\cdot}436518521 \times 10^{-1}$
$C_2 = 1{\cdot}428945805 \times 10^{-2}$
$C_3 = 2{\cdot}650648471 \times 10^{-4}$
$C_4 = 3{\cdot}031240396 \times 10^{-6}$
$C_5 = 2{\cdot}034080948 \times 10^{-8}$
$C_6 = 6{\cdot}136820929 \times 10^{-11}$.

The maximum departure from Goff–Gratch over the range — 40 °C to + 50 °C is — 1·264 × 10^{-2} mb and occurs at + 50 °C.

For an ice surface from — 50 °C to 0 °C:

$C_0 = 6{\cdot}109177956$
$C_1 = 5{\cdot}03469897 \times 10^{-1}$
$C_2 = 1{\cdot}886013408 \times 10^{-2}$
$C_3 = 4{\cdot}176223716 \times 10^{-4}$
$C_4 = 5{\cdot}824720280 \times 10^{-6}$
$C_5 = 4{\cdot}838803174 \times 10^{-8}$
$C_6 = 1{\cdot}838826904 \times 10^{-10}$.

These coefficients will give e_i, the saturation vapour pressure in millibars with respect to a plane surface of pure ice.

Vapour pressure

To compute the ambient vapour pressure of the air, the psychrometric equation is used:

$$e = e_w' - AP(T - T_w), \quad \ldots \quad (8)$$

where e = ambient vapour pressure in millibars,
e_w' = saturation vapour pressure in millibars with reference to water at the wet-bulb temperature,
A = the psychrometric coefficient,
P = atmospheric pressure in millibars,
T = dry-bulb temperature in degrees Celsius,
T_w = wet-bulb temperature in degrees Celsius.

The value of A is dependent on, among other things, the ventilation rate past the wet-bulb thermometer. For Meteorological Office pattern mercury-in-glass thermometers in a standard thermometer screen with natural ventilation a value of 0·000799 is used. For psychrometers of the Assmann type with forced ventilation of 3 to 5 m s^{-1} a value of 0·000667 is used. For practical purposes for readings from a fixed location at or near sea level, variations in atmospheric pressure may be ignored and P is taken as 1000 mb. Equation (8) thus reduces to

$$e = e_w' - 0{\cdot}799(T - T_w) \quad \ldots \quad (9)$$

for naturally ventilated psychrometers and

$$e = e_w' - 0{\cdot}667(T - T_w) \quad \ldots \quad (10)$$

for Assmann-type forced ventilation psychrometers.

Relative humidity

Relative humidity is defined (World Meteorological Organization, 1975) by

$$U = 100\ (e/e_d) \text{ per cent}, \quad \ldots \quad (11)$$

where e = ambient vapour pressure in millibars, and
e_d = saturation vapour pressure in millibars with respect to water at the same pressure and temperature.

Computation of dew-point temperature

The dew-point temperature of a sample of air is defined as the temperature to which the sample must be cooled at constant pressure in order that the sample shall be saturated with respect to a plane surface of pure water. Thus the vapour pressure of the sample is the saturation vapour pressure at the dew-point temperature. If the ambient vapour pressure is known it is required to determine the temperature for which that is the saturation vapour pressure.

There is a variety of methods, based on the above equations for saturation vapour pressure, by which the dew-point temperature may be calculated. The Goff–Gratch equation is not amenable to easy solution for temperature, although for determining the accuracy of other methods it is possible by means of a reiterative trial and error method. This is very costly in terms of computing time.

Richards. Richards's equation (equation (6)) can be solved by an iterative process as follows:

Form a first estimate of t by neglecting all but the first term in equation (6); that is

$$t_1 = \frac{\ln (e/1013{\cdot}25)}{13{\cdot}3185} \qquad (e = \text{vapour pressure in millibars}).$$

Successively more accurate estimates of t are obtained from

$$t_{n+1} = t_1 + [(0{\cdot}1299t_n + 0{\cdot}6445)t_n + 1{\cdot}976]\, t_n^2/13{\cdot}3185,\ n = 1, 2, \ldots$$

When the difference between successive estimates is suitably small the desired estimate of T_d (dew-point temperature) is found from

$$T_d = 373{\cdot}15/(1 - t_{n+1}).$$

For accuracy within the limitations of normal thermometry the difference between successive estimates should be less than 10^{-8}.

Lowe. Lowe's polynomial (equation (7)) can be solved using the Newton–Raphson approximation method. This states that if q_n is an approximation to a root of a polynomial $F(x)$ then a better approximation q_{n+1} is given by

$$q_{n+1} = q_n - F(x)/F'(x),$$

where $F'(x)$ is the first derivative of $F(x)$.

The initial approximation, q_1, can be made by subtracting the wet-bulb depression from the wet-bulb temperature (e.g. dry bulb = 10 °C, wet bulb = 7 °C; then first approximation to $q = 7 - (10 - 7) = 4$ °C). Then

$$q_{n+1} = q_n - \frac{[(C_0 - e) + C_1q_n + C_2q_n^2 + \ldots + C_6q_n^6]}{(C_1 + 2C_2q_n + 3C_3q_n^2 + \ldots + 6C_6q_n^5)} \ldots \qquad (12)$$

As successive approximations to q approach the limiting value the expression in the square brackets in equation (12) approaches zero and when it has become suitably small (less than 10^{-8}) q_{n+1} may be taken as the dew-point temperature.

Hooper. Hooper has developed a sixth-order polynomial to compute temperatures from saturation vapour pressures. This is claimed to be valid from − 40 °C to + 50 °C.

$$T = n_0 + n_1V + n_2V^2 + n_3V^3 + n_4V^4 + n_5V^5 + n_6V^6, \qquad (13)$$

where T = temperature in degrees Celsius

V = natural logarithm of the saturation vapour pressure in millibars

$$n_0 = -2{\cdot}25949867 \times 10^1$$
$$n_1 = 1{\cdot}133464632 \times 10^1$$
$$n_2 = 5{\cdot}754465709 \times 10^{-1}$$
$$n_3 = 2{\cdot}999976429 \times 10^{-2}$$
$$n_4 = 1{\cdot}971073756 \times 10^{-3}$$
$$n_5 = 3{\cdot}369657915 \times 10^{-5}$$
$$n_6 = 1{\cdot}384040269 \times 10^{-5}.$$

The maximum departure from Goff–Gratch is $1{\cdot}40 \times 10^{-3}$ °C at + 50 °C over the range — 40 °C to + 50 °C.

Hooper's coefficients can again be adjusted to give a closer approximation to the Goff–Gratch results:

$$n_0 = -2{\cdot}259529963 \times 10^1$$
$$n_1 = 1{\cdot}133418988 \times 10^1$$
$$n_2 = 5{\cdot}756940348 \times 10^{-1}$$
$$n_3 = 3{\cdot}025080051 \times 10^{-2}$$
$$n_4 = 1{\cdot}778276954 \times 10^{-3}$$
$$n_5 = 7{\cdot}443287646 \times 10^{-5}$$
$$n_6 = 1{\cdot}129170314 \times 10^{-5}.$$

These coefficients give a maximum departure from Goff–Gratch of $1{\cdot}11 \times 10^{-4}$ °C at + 50 °C over the range — 40 °C to + 50 °C.

Polynomial in e. It is possible to form a polynomial that approximates the curve of temperature against saturation vapour pressure with respect to water. A sixth-order polynomial is required to obtain an accuracy within the limits of normal thermometry over the range — 10 °C to +35 °C.

$$T_d = A_0 + A_1 + A_2e^2 + A_3e^3 + A_4e^4 + A_5e^5 + A_6e^6, \qquad (14)$$

where T_d = dew-point temperature in degrees Celsius
e = ambient vapour pressure in millibars
$$A_0 = -2{\cdot}298609588 \times 10^1$$
$$A_1 = 5{\cdot}639954495$$
$$A_2 = -4{\cdot}058494504 \times 10^{-1}$$
$$A_3 = 1{\cdot}839604600 \times 10^{-2}$$
$$A_4 = -4{\cdot}669899615 \times 10^{-4}$$
$$A_5 = 6{\cdot}085695266 \times 10^{-6}$$
$$A_6 = -3{\cdot}160820732 \times 10^{-8}.$$

The maximum departure from Goff–Gratch over the range is $-3{\cdot}757 \times 10^{-1}$ °C at + 33·9 °C.

Straight-line approximations. The foregoing procedures are capable of giving accuracies within the limits of normal thermometry and, in the case of the logarithmic polynomials, considerably better. However, there may be applications where such a high degree of accuracy is not required and where ease of computation is a higher priority. For these applications it is possible to fit a series of straight lines to the curve of saturation vapour pressure against temperature. To achieve an accuracy of approximately ± 0·3 °C in dew-point temperature over the temperature range — 10 °C to + 35 °C nine straight lines are required. These are of the form

$$e_w = B_0 + B_1T, \qquad (15)$$

where e_w = saturation vapour pressure in millibars with respect to a plane surface of pure water at temperature T,

T = temperature in degrees Celsius

and

T °C	B_0	B_1	e_w mb
−10 to −5	+ 5·5388	0·2709	2·9 to 4·2
−5 to 0	+ 6·0673	0·3792	4·2 to 6·1
0 to +5	+ 6·0506	0·5231	6·1 to 8·7
+5 to +10	+ 5·0874	0·7116	8·7 to 12·3
+10 to +15	+ 2·6232	0·9554	12·3 to 17·0
+15 to +20	− 2·0835	1·2671	17·0 to 23·4
+20 to +25	− 9·9993	1·6610	23·4 to 31·7
+25 to +30	−22·3562	2·1535	31·7 to 42·4
+30 to +35	−40·6943	2·7630	42·4 to 56·2

Equation (15) may be rearranged thus:

$$T = \frac{e_w - B_0}{B_1}, \text{ or } T_d = \frac{e - B_0}{B_1}, \quad \ldots\ldots\ldots\ldots\ldots\ldots\ldots \quad (16)$$

to give dew-point temperature from ambient vapour pressure.

Dew-point temperature from relative humidity. The following expression will give dew-point temperature from values of relative humidity and dry-bulb temperature. It is reasonably accurate at high humidities with dry-bulb temperatures near to + 20 °C, but accuracy falls off quite rapidly as the relative humidity falls and the dry-bulb temperature departs from 20 °C.

$$T_d = T - K_0 + K_1 U, \quad \ldots\ldots\ldots\ldots\ldots\ldots\ldots \quad (17)$$

where T_d = dew-point temperature in degrees Celsius,

T = dry-bulb temperature in degrees Celsius, and

U = relative humidity, per cent

and

U	K_0	K_1
100 to 65 per cent	17·9	0·18
65 to 45 per cent	22·5	0·25

More accurate results are obtained from

$$T_d = U(0{\cdot}198 + 0{\cdot}0017T) + 0{\cdot}84T - 19{\cdot}2. \quad \ldots\ldots\ldots\ldots\ldots \quad (18)$$

This gives dew-point temperatures within 1 °C of the true value over ranges of dry-bulb temperature and relative humidity 0 °C to + 30 °C and 100 per cent to 40 per cent, respectively.

Practical procedures

There are numerous ways of calculating the desired humidity variables of the air given the dry- and wet-bulb temperatures. The method used will depend on the accuracy required, the calculating facilities available and the preference of the user.

For all calculations it is necessary to compute the saturation vapour pressure at the wet-bulb temperature and this may be done using one of equations (1), (3), (5), (6) or (7) or the straight-line approximations—equation (15). The ambient vapour pressure may then be computed using equation (9) or (10).

If relative humidity is required, saturation vapour pressure at the dry-bulb temperature is computed, again from equations (1), (3), (5), (6), (7) or (15), and relative humidity is then found by means of equation (11).

If dew-point temperature is required the iterative solution of Richards's approximation or of Lowe's approximation, or the use of Hooper's polynomial (equation (13)) give the most accurate results. Alternatively the polynomial in e (equation (14)) or the straight-line approximation (equation (16)) may be used, giving a lower degree of accuracy.

If dry-bulb temperature and relative humidity are given, equations (17) and (18) will give a value of dew-point temperature if great accuracy is not important.

Comparison of methods

In order to compare one method against another the Goff–Gratch results were taken as standard and other methods compared with them.

Table I gives values of mean relative difference, root-mean-square relative difference and maximum difference from Goff–Gratch for Hooper's, Hooper's with Sargent's coefficients, Richards's, Lowe's and straight-line approximations for saturation vapour pressure from temperature.

Table II gives similar values for Richards's, the Newton–Raphson solution of Lowe's polynomial, Hooper's, Hooper's with Sargent's coefficients, the polynomial in e and straight-line methods of obtaining temperature from values of saturation vapour pressure.

The values in Tables I and II were computed over the stated range of temperature at 0·1 °C increments.

Table I. *Comparison of computation methods for saturation vapour pressure from temperature against Goff–Gratch*

Method	Range of temperature	Mean relative difference	Root-mean-square relative difference	Maximum relative difference
	degrees Celsius		*millibars*	
Hooper	—40 to + 50	$1{\cdot}564 \times 10^{-5}$	$4{\cdot}087 \times 10^{-5}$	$2{\cdot}106 \times 10^{-4}$ at —40·0 °C
Sargent	—40 to + 50	$-3{\cdot}889 \times 10^{-6}$	$5{\cdot}016 \times 10^{-6}$	$-1{\cdot}522 \times 10^{-6}$ at +50·0 °C
Richards	—40 to + 50	$1{\cdot}495 \times 10^{-4}$	$3{\cdot}369 \times 10^{-4}$	$7{\cdot}819 \times 10^{-4}$ at —34·3 °C
Lowe	—40 to + 50	$3{\cdot}079 \times 10^{-4}$	$7{\cdot}711 \times 10^{-4}$	$2{\cdot}408 \times 10^{-3}$ at —33·5 °C
Straight-line approximations	—10 to + 35	$-1{\cdot}485 \times 10^{-3}$	$4{\cdot}134 \times 10^{-3}$	$1{\cdot}149 \times 10^{-2}$ at —35·0 °C

Table II. *Comparison of computation methods for temperature from saturation vapour pressure against Goff–Gratch*

Method	Range of temperature	Mean relative difference	Root-mean-square relative difference	Maximum relative difference
		degrees Celsius		
Richards	—40 to +50	$4{\cdot}141 \times 10^{-3}$	$5{\cdot}629 \times 10^{-3}$	$-3{\cdot}971 \times 10^{-3}$ at +50 °C
Lowe	—40 to +50	$3{\cdot}218 \times 10^{-3}$	$8{\cdot}013 \times 10^{-3}$	$3{\cdot}739 \times 10^{-3}$ at —12 °C
Hooper	—40 to +50	$-1{\cdot}349 \times 10^{-4}$	$4{\cdot}518 \times 10^{-4}$	$1{\cdot}401 \times 10^{-3}$ at +50 °C
Sargent	—40 to +50	$5{\cdot}750 \times 10^{-5}$	$6{\cdot}396 \times 10^{-5}$	$1{\cdot}113 \times 10^{-4}$ at +50 °C
Polynomial in e	—10 to +35	$5{\cdot}587 \times 10^{-3}$	$1{\cdot}317 \times 10^{-1}$	$-3{\cdot}757 \times 10^{-1}$ at +33·9 °C
Straight-line approximations	—10 to +35	$2{\cdot}285 \times 10^{-2}$	$5{\cdot}938 \times 10^{-2}$	$-1{\cdot}214 \times 10^{-1}$ at —10 °C

References

Clenshaw, C. W. 1960 Curve fitting with a digital computer. *Comp J*, **2**, 170–173.

Goff, J. A. 1965 Saturation pressure of water on the new Kelvin scale. *In* Wexler, A. (editor); Humidity and moisture, Vol. 3. New York, Reinhold Publishing Corporation, 289–292.

Goff, J. A. and Gratch, S. 1945 Thermodynamic properties of moist air. *Trans Am Soc Heat Vent Eng*, **51**, 125–157.

Lowe, P. R. 1977 An approximating polynomial for the computation of saturation vapour pressure. *J Appl Meteorol*, **16**, 100–103.

Powell, M. J. D. 1965 A method for minimizing a sum of squares of non-linear functions without calculating derivatives. *Comp J*, **7**, 303–307.

Richards, H. M. 1971 A simple expression for the saturation vapour pressure of water in the range —50 to 140 °C. *J Phys*, D, *Appl Phys*, **4**, L15–L18.

World Meteorological Organization 1975 Technical regulations, Vol. 1. Geneva, WMO No. 49, [A.2.2.] 1.1.2.

551.5(09):551.508:069

The Museum of Meteorological Instruments

By J. P. Jay

(Meteorological Office, Bracknell)

'The thing that hath been, it is that which shall be; and that which is done is that which shall be done: and there is no new thing under the sun.'

Ecclesiastes 1:9.

Anyone seeking to prove the wisdom of this well-known quotation might be advised to visit the Museum of Meteorological Instruments (Plate II). There he will find many examples of old instruments, the principles and often the looks of which are disconcertingly similar to those of current models. This, the Meteorological Office's own Museum, was opened in December 1979, in Room 402 (off the Staff Restaurant) in the Headquarters Building at Bracknell. It is open for viewing during normal working hours when Meteorological Office staff are at liberty to walk round at leisure. Members of the general public may also be shown round on application at the main entrance.

It is very important that steps should be taken to preserve examples of instruments before they disappear for ever. Apart from their obvious interest value, it is often very useful for designers to be able to refer to what has gone before; a look at the real thing can be far more helpful than drawings and many pages of descriptive writing. The present collection is just a beginning. The exhibits will increase in number as the years go by. Now that the initiative has been taken, it is to be hoped that all those who have meteorological instruments in their care will ensure that any of an old or interesting nature will be offered to the Museum before being disposed of elsewhere. If contact is made with Met 0 16c, arrangements will be made to collect anything suitable.

The instruments on display include many which are worthy of special mention. Impressive at the far end of the room, stands the massive Beckley–Robinson anemograph which was installed on the roof

of the Radcliffe Observatory, Oxford, in 1893 (Plate III). It worked so reliably and effectively that it was in constant use for 83 years until 1976 and the clock mechanism still functions perfectly. It is on permanent loan from the University of Oxford School of Geography. This piece of equipment was designed by Robert Beckley, of Kew Observatory, in 1856. He used the cup anemometer originated by Dr Thomas Romney Robinson, the Irish astronomer, some ten years earlier. The characteristic direction mechanism was based on the windmill governor invented by Follet Osler. This gives a much steadier indication of wind direction than a plain wind vane and Beckley improved Osler's design by using two windmills instead of one.

In the case alongside will be seen an original early prototype model which was constructed by Beckley himself (Plate IV). The modern Mk 4E wind vane adjacent to it looks remarkably similar, showing how difficult it is, even in this modern age, to improve on the work of the 'old masters' (Plate V).

It is not generally realized that the tipping-bucket rain-gauge dates back as far as 1660 when no less a person than Sir Christopher Wren used the system. The principle has survived the years and remains the basis of quite sophisticated modern instruments. Various examples are on show. Of particular interest is the Negretti & Zambra improved self-recording rain-gauge (*c.* 1890) which was kindly presented to us by the East Devon District Council (Plate VI). This unit was in regular use at the Sidmouth climatological station until 1973. In this device each tip of the buckets, holding 0·01 inch, advances an escapement wheel and a trace is made on the drum of a clockwork recorder. Another recording rain-gauge of about the same age is the Negretti & Zambra dial rain-gauge where tips are mechanically transmitted to a pointer and dial in 0·01 inch increments (Plate VII).

In the field of humidity measurement we have examples of dew-point hygrometers such as Daniell's (1860) (Plate VIII), G. Dines's and Regnault's (1875), all of which use methods of cooling a glass surface so that the temperature at which condensation occurs may be observed. Today's dew-point hygrometers do exactly the same but with automatic optical aids to perform the observation. Horace Benedict de Saussure, of Geneva, first suggested the use of human hair for determining humidity. An interesting example of an early hair hygrometer by Bate (*c.* 1830) is on display. It hardly needs to be pointed out that Meteorological Office hygrographs in 1980 operate on the same principle. In the novelty class and not, to my knowledge, copied today, is Kater's hygrometer (*c.* 1812) (Plate IX); this takes advantage of the twisting action of the seed awn of the grass *Andropon contortum* to operate a pointer over a graduated dial.

Wet- and dry-bulb thermometers are still the 'standard' for humidity observations and have been in use for some considerable time. The fact that a wet thermometer bulb gives a lower reading than a dry one was first noted by William Cullen, a Scot, in 1777. It was not until 1792 that James Hutton, a compatriot, used the principle for hygrometry. Dr Abraham Mason produced his well-known psychrometer in 1836 and the Museum has a neat example dated around 1870. An instrument for remote wet- and dry-bulb observations is the Negretti & Zambra recording thermometer (*c.* 1898) (Plate X). This incorporates an electrical system, actuated by a clock, to 'flip over' a pair of constricted thermometers and thus hold their readings so that observations for a specific time can be taken at leisure.

Another early instrument, obviously intended for remote use, is the Goldschmid barograph (1880) (Plate XI). This has an aneroid capsule stack and a clock mechanism. At hourly intervals indentations are punched on to a paper roll from which pressures can be read off later, using a calibrated scale. Aneroid capsules still dominate the techniques of practical barometry, having almost entirely pushed out the once-supreme liquid types. On the left as one enters the Museum is the top part of the 1873 Jordan glycerine barometer (Plate XII) which was installed in the office of *The Times* at Printing House

Square, London, until about 1957. As the tube was some 30 feet long, the cistern would have been housed two or three floors below. The readings were plotted on weekly charts in the very substantial shuttered cabinet alongside. The record displayed is presumably the last one made before the equipment was abandoned. The resolution of this barometer was apparently very fine and one wonders whether adequate practical use could ever have been made of the information. The oldest and most treasured item in our collection is the mercury barometer by Dan Quare (*c.* 1695) (Plate XIII). This superb instrument, which is still in good working order, is truly a fitting memorial to the craftsmanship of the period. It is currently kept in the office of the Assistant Director (Operational Instrumentation) at Beaufort Park, where it may be seen by arrangement with his personal assistant. Other interesting articles at present housed outside the Museum itself include a Dines's improved hygrometer and a set of genuine African rain-making stones which are in the Director-General's office.

Much has been written about the FitzRoy storm glass but no one has yet ventured any explanation of how it works. I do not intend to break with that tradition, but we have reconstructed one, using a formula handed down through the years. Although it is housed in the relatively stable environment of the display cabinet, regular visitors will see that interesting changes in the crystalline formations do take place. It has, so far, been impossible to relate these clearly to weather changes for prognostic purposes as Admiral FitzRoy so confidently did. Its presence in the Museum takes us back hundreds of years to the days of the old alchemists and the times when interest in instruments to assist attempts to monitor and forecast the weather was just beginning. Perhaps our instrument designers of today may take heart from the progress that has been made and whilst not forgetting the well-tried principles, nevertheless realize that there is ample room for many really new developments for the sun to shine on.

Review

A short course in cloud physics (*second edition*), by R. R. Rogers. 215 mm × 150 mm, pp. viii + 235, *illus*. Pergamon Press, Oxford, New York, Toronto, Sydney, Paris, Frankfurt, 1979. Price (flexicover) US $12.50, £6.25 (hardback available at US $25.00, £12.50).

The first edition of this monograph was published some four years ago and assessed by the present reviewer (*Meteorol Mag*, **105**, 1976, pp. 216–217). Some minor errors have been corrected in the second edition. Thus the values given for a number of constants and parameters of interest are now in keeping with those of standard tables. Greater consistency in the use of SI units is apparent; nevertheless some lapses remain. A small amount of new material has been added in the sections on condensation and ice nucleation. Derivations of the condensational and coalescence growth equations have been recast. However, the major improvement is the provision of hints to solutions and answers for alternate problems set at the end of each chapter. This corrects a rather obvious deficiency and almost certainly increases the value of the book as a teaching aid.

It must be admitted that a criticism levelled at the first edition has not been fully justified in practice. It was suggested that the book was unlikely to provide a text for students which was comprehensive enough to be a useful addition to the standard works. Whilst some further expansion of the sections dealing with theoretical developments would be an advantage, the reviewer's copy of the first edition has been consulted frequently as an *aide-mémoire*. Rogers has succeeded in distilling much that is of practical value in the subject.

P. Ryder

THE METEOROLOGICAL MAGAZINE

No. 1297 August 1980 Vol. 109

CONTENTS

Page

An aircraft-mounted pyranometer. A. P. Cluley and J. P. Cowley 217

An investigation into the variations of grass-minimum depressions. M. N. Pickup 230

Computation of vapour pressure, dew-point and relative humidity from dry- and wet-bulb temperatures. G. P. Sargent 238

The Museum of Meteorological Instruments. J. P. Jay 246

Review

A short course in cloud physics (second edition). R. R. Rogers. *P. Ryder* 248

NOTICES

It is requested that all books for review and communications for the Editor be addressed to the Director-General, Meteorological Office, London Road, Bracknell, Berkshire RG12 2SZ, and marked 'For Meteorological Magazine'.

The responsibility for facts and opinions expressed in the signed articles and letters published in this magazine rests with their respective authors.

Complete volumes of 'Meteorological Magazine' beginning with Volume 54 are now available in microfilm form from University Microfilms International, 18 Bedford Row, London WC1R 4EJ, England.

Full size reprints of out-of-print issues are obtainable from Johnson Reprint Co. Ltd., 24–28 Oval Road, London NW1 7DX, England.

Issues in Microfiche starting with Volume 58 may be obtained from Johnson Associates Inc., P.O. Box 1017, Greenwich, Conn. 06830, U.S.A.

© *Crown copyright* 1980

Printed in England by Heffers Printers Ltd, Cambridge
and published by
HER MAJESTY'S STATIONERY OFFICE

£1.60 monthly
Dd. 698260 K15 8/80

Annual subscription £21.18 including postage
ISBN 0 11 722064 7
ISSN 0026–1149